

# AAPG Bulletin

## Petroleum generation timing and source in the Northern Longmen Shan Thrust Belt, Southwest China: Implications for multiple oil generation episodes and sources --Manuscript Draft--

<b>Manuscript Number:</b>	BLTN17-125
<b>Full Title:</b>	Petroleum generation timing and source in the Northern Longmen Shan Thrust Belt, Southwest China: Implications for multiple oil generation episodes and sources
<b>Article Type:</b>	Article
<b>Keywords:</b>	Re-Os geochronology Organic Geochemistry Petroleum evolution Northern Longmen Shan Thrust Belt
<b>Corresponding Author:</b>	Chuanbo Shen China university of Geosciences, Wuhan Wuhan, Hubei CHINA
<b>Corresponding Author Secondary Information:</b>	
<b>Corresponding Author's Institution:</b>	China university of Geosciences, Wuhan
<b>Corresponding Author's Secondary Institution:</b>	
<b>First Author:</b>	Xiang Ge
<b>First Author Secondary Information:</b>	
<b>Order of Authors:</b>	Xiang Ge Chuanbo Shen David Selby Jie Wang Liangbang Ma Xiaoyan Ruan Shouzhi Hu Lianfu Mei
<b>Order of Authors Secondary Information:</b>	
<b>Manuscript Region of Origin:</b>	CHINA
<b>Abstract:</b>	<p>The temporal evolution of hydrocarbons (~500 million barrels oil) and its relationship to the orogenic events of the Longmen Shan Thrust Belt have been extensively debated. The hydrocarbons occur as solid bitumen, as dykes and/or coatings within/along faults/fractures, and as present day oil seeps. Here utilizing organic geochemistry, we demonstrate that all the bitumen exhibit similar organo-gechemical characteristics, and were sourced from the Late Neoproterozoic-Early Cambrian Doushantuo and Qiongzhusi formations. In contrast, the organic geochemistry of the present day oil seeps are distinct from that of the bitumen, and suggest that the source is the Permian Dalong Formation.</p> <p>Bitumen rhenium-osmium data indicate that the Late Neoproterozoic-Early Cambrian Doushantuo and Qiongzhusi formations underwent two temporally distinct oil generation events; initially during the Early Ordovician (ca.486 Ma) prior to the Caledonian Orogeny, and secondly during the Jurassic (ca.165 Ma) coinciding with the Indosinian-Yanshan orogenies. In contrast, the rhenium-osmium data of the present day oil seeps are too similar to yield a meaningful age, although the source is considered to have underwent hydrocarbon maturation between the Triassic and Jurassic. The temporal hydrocarbon evolution in the the Longmen Shan Thrust Belt</p>

	also provides implication for the hydrocarbon evolution and future exploration of the adjacent petroliferous Sichuan Basin.
<b>Suggested Reviewers:</b>	Huaning Qiu qiuhn@gig.ac.cn
	Bruce Schaefer Bruce.Schaefer@mq.edu.au
	Naveen Hakhoo naveen@jugaa.com
	Svetoslav Georgiev georgiev@colostate.edu
	Simon Kelley simon.kelley@open.ac.uk
<b>Opposed Reviewers:</b>	Holly Stein holly.stein@colostate.edu We ask that given the publication history between the Colorado State Group and that we are working on very similar topics that this paper is not reviewed by this research group (from Colorado State)
<b>Additional Information:</b>	
<b>Question</b>	<b>Response</b>

1 **This is a revised version with the manuscript Number BLTN16-230**

2

3 **Petroleum generation timing and source in the Northern Longmen**  
4 **Shan Thrust Belt, Southwest China: Implications for multiple oil**  
5 **generation episodes and sources**

6

7 **Xiang Ge<sup>1,2</sup>, Chuanbo Shen<sup>1\*</sup>, David Selby<sup>1,2</sup>, Jie Wang<sup>3</sup>, Liangbang Ma<sup>3</sup>, Xiaoyan Ruan<sup>1</sup>,**  
8 **Shouzhi Hu<sup>1</sup>, Lianfu Mei<sup>1</sup>**

9

10 <sup>1</sup>Key Laboratory of Tectonics and Petroleum Resources (China University of Geosciences),  
11 Ministry of Education, Wuhan, 430074, China

12 <sup>2</sup>Department of Earth Sciences, Durham University, Durham, DH1 3LE, UK

13 <sup>3</sup>Wuxi institute of petroleum geology, SINOPEC, Wuxi, 214151, China

14 **\*Corresponding author E-mail: [cugshen@126.com](mailto:cugshen@126.com)**

15

## 16 **Acknowledgement**

17 This work was supported by the National Natural Science Foundation of China (No.  
18 41372140, 41672140, 40902038) and the Fundamental Research Fund for the Central  
19 Universities, China University of Geosciences (Wuhan, No. 201536), 111 project (No.  
20 B14031), the Outstanding Youth Funding of Natural Science Foundation of Hubei  
21 Province (No. 2016CFA055), the Wuhan Science and Technology Project (No.  
22 2016070204010145), the PetroChina Innovation Foundation (No. 2016D-5007-0103)  
23 and a China Scholarship Council (CSC) postgraduate award to Xiang Ge. Selby  
24 acknowledges the TOTAL Endowment Fund. We thank Barry J. Katz, Naveen Hakhoo,

25 Svetoslav Georgiev, Professor Liu, and Rachael Bullock for their constructive  
26 comments.

27 **Abstract**

28 The temporal evolution of hydrocarbons (~500 million barrels oil) and its relationship to  
29 the orogenic events of the Longmen Shan Thrust Belt have been extensively debated.  
30 The hydrocarbons occur as solid bitumen, as dykes and/or coatings within/along  
31 faults/fractures, and as present day oil seeps. Here utilizing organic geochemistry, we  
32 demonstrate that all the bitumen exhibit similar organo-gechemical characteristics, and  
33 were sourced from the Late Neoproterozoic–Early Cambrian Doushantuo and  
34 Qiongzhusi formations. In contrast, the organic geochemistry of the present day oil  
35 seeps are distinct from that of the bitumen, and suggest that the source is the Permian  
36 Dalong Formation.

37 Bitumen rhenium-osmium data indicate that the Late Neoproterozoic–Early Cambrian  
38 Doushantuo and Qiongzhusi formations underwent two temporally distinct oil  
39 generation events; initially during the Early Ordovician (ca.486 Ma) prior to the  
40 Caledonian Orogeny, and secondly during the Jurassic (ca.165 Ma) coinciding with the  
41 Indosinian-Yanshan orogenies. In contrast, the rhenium-osmium data of the present day  
42 oil seeps are too similar to yield a meaningful age, although the source is considered to  
43 have underwent hydrocarbon maturation between the Triassic and Jurassic. The  
44 temporal hydrocarbon evolution in the the Longmen Shan Thrust Belt also provides  
45 implication for the hydrocarbon evolution and future exploration of the adjacent  
46 petroliferous Sichuan Basin.

47

48 **1. Introduction**

49 Source rock burial and maturation history, coupled with hydrocarbon generation and  
50 subsequent migration are key factors of a petroleum system, which are often temporally

51 associated with regional tectonic events (Bordenave and Hegre, 2005; Moretti et al.,  
52 1996; Urien et al., 1995; Yahi et al., 2001). For example, (1) in the Berkine (Ghadames)  
53 Basin, eastern Algeria, hydrocarbon maturation of the Silurian, Llandoveryian –  
54 Wenlockian source rock and associated oil generation directly relates to the timing of the  
55 Cretaceous African Orogeny (Yahi et al., 2001), and (2) in the foreland of the Sub  
56 Andean Zone in Bolivia, three stages of tectonic accretion are suggested to have  
57 controlled three phases of sedimentation and oil generation during the Cenozoic  
58 (Moretti et al., 1996; Urien et al., 1995).

59 The key to understanding the direct relationship between tectonism and the evolution of  
60 a petroleum system are the accurate estimates for the timing of the related tectonism and  
61 that of the hydrocarbon generation, expulsion and accumulation. Recent successes in  
62 determining age constraints and the relationship between tectonism and petroleum  
63 evolution has been achieved through the application of both radiometric (e.g., Re-Os,  
64 Ar-Ar, Apatite Fission Track (AFT)) and indirect techniques (e.g., basin/tectonic  
65 models) (Boles et al., 2004; Fall et al., 2015; Ge et al., 2016).

66 The Sichuan Basin in the South China Block records multiple tectonic events (e.g.,  
67 Ordovician-Devonian Caledonian, Late Triassic Indosinian, Late Jurassic Yanshan, and  
68 the Cenozoic Himalaya orogenies) (Chen and Wilson, 1996; Dai et al., 2009;  
69 Harrowfield and Wilson, 2005; Jin et al., 2010; Sun, 2011; Yan et al., 2011). The  
70 majority of the hydrocarbon reserves of the Sichuan Basin are distributed close to its  
71 border regions (e.g., Longmen Shan Thrust belt, Micang Shan Uplift, Daba Shan  
72 Orogenies) (Li et al., 2015; Li et al., 2001; Liu et al., 2011; Ma et al., 2010) (Fig. 1B).

73 The basin has current reserve estimates of ~30 Bbbl (billions of barrels) of oil and ~180  
74 Tcf (Trillion cubic feet) of gas (Zhang and Zhu, 2006; Zou et al., 2014a). Key examples

75 are the giant Puguang Gas field that is located adjacent to the Daba Shan orogenic belt  
76 in the northeast Sichuan Basin which possesses ~12 proven original in-place Tcf gas  
77 (Ma et al., 2007b), the great Yuanba gas field (~2 Tcf proven gas) that lies near the  
78 Micang Shan Uplift in the northern Sichuan Basin (Liu et al., 2011), and several gas  
79 fields possessing ~1 Tcf gas (e.g., Dayi, Majing and Pingluoba) that occur near the  
80 Longmen Shan Thrust belt (Liu et al., 2011) (Fig. 1B). In addition to the gas fields in  
81 the Longmen Shan Thrust belt, hydrocarbons are present as bitumen. The total bitumen  
82 accumulation, which is recoverable is estimated to yield a reserve in excess of 500  
83 million barrels (Mbbbl) of oil (Liu et al., 2003).

84 The Longmen Shan Thrust belt is located between the Songpan-Ganze Terrane and the  
85 Sichuan Foreland Basin, and marks the western margin of the Sichuan Basin (Fig. 1A).  
86 The belt is tectonically complex due to multiple orogenic events from the Palaeozoic to  
87 present (Caledonian, Indosinian–Yanshan, Himalaya) (Jin et al., 2010; Yan et al., 2003).  
88 Abundant hydrocarbons predominantly occur in Neoproterozoic to Permian strata and  
89 are typically spatially associated with thrust faults and associated fracture systems (Fig.  
90 1C) (Dai et al., 2009; Huang and Wang, 2008; Liu et al., 2003). To date, the origin, age  
91 and the evolution of the hydrocarbons is debated. For example, either organic-rich strata  
92 of the Late Neoproterozoic–Early Cambrian (Dai et al., 2009; Liu et al., 2009; Tian,  
93 2009; Wei et al., 2008; Xie et al., 2003) or Permian (Liu et al., 2003; Rao et al., 2008;  
94 Wang et al., 1997) are considered to be the main source rocks. Additionally, basin burial  
95 history and fluid inclusion analyses propose multiple hydrocarbon generation and  
96 migration events, e.g., between the Ordovician and Silurian (Wang and Li, 1999; Wei et  
97 al., 2008) and during the Late Triassic (Liu et al., 2009), as well as during the Cenozoic  
98 (Liu et al., 2003; Rao et al., 2008).

99 As a petroleum component, bitumen records significant information regarding  
100 petroleum evolution, including hydrocarbon generation, migration, accumulation and  
101 alteration (Hwang et al., 1998; Parnell and Swainbank, 1990; Selby et al., 2005;  
102 Summons et al., 2008; Zhu et al., 2001). Recently, Re-Os isotope dating of oil and  
103 bitumen has shown good potential for determining the absolute timing of hydrocarbon  
104 generation (Cumming et al., 2014; Finlay et al., 2011; Ge et al., 2016; Georgiev et al.,  
105 2016; Lillis and Selby, 2013; Selby and Creaser, 2005; Selby et al., 2005; Selby et al.,  
106 2007). In this study, we present new Re-Os data and organic geochemistry of bitumen  
107 and present day oil seeps from the Northern Longmen Shan Thrust belt. The data are  
108 discussed with the previous hydrocarbon evolution knowledge, as well as U-Pb, Ar-Ar  
109 and Apatite Fission Track (AFT) dates that constrain the timings of tectonism to  
110 understand the petroleum evolution and its relationship with tectonism. Our data  
111 provide not only an improved understanding of the petroleum evolution within the  
112 Longmen Shan Thrust belt, but also provides implications for the potential utility of Re-  
113 Os hydrocarbon chronometer to help constrain the absolute timing of both hydrocarbon  
114 generation and associated tectonism in petroleum systems worldwide.

115

## 116 **2. Geological Setting**

117 The NE-SW striking Longmen Shan Thrust belt is ~500 km long and ~50 km wide. The  
118 belt is bordered by the Micang Shan uplift to the north, the Kangdian paleo uplift to the  
119 South, the Songpan-Garze Belt to the west, and the Sichuan Basin to the east (Burchfiel  
120 et al., 1995; Dirks et al., 1994; Jin et al., 2010) (Fig. 1C). Longitudinally, the Longmen  
121 Shan Thrust belt is divided into three sub-structural belts by four major faults: the  
122 Maoxian-Wenchuan, Beichuan-Yingxiu, Anxian-Dujiangyan and the Guangyuan-Dayi



123 faults (Fig. 1C). Further, the belt can also be separated geographically into three areas:  
124 the northern, middle and southern segments (Fig. 1C) (Chen and Wilson, 1996; Deng et  
125 al., 2012; Jin et al., 2010; Li et al., 2008; Liu et al., 2016; Wang et al., 2015; Yan et al.,  
126 2011).

127 The Longmen Shan Thrust belt has experienced a complex tectonic evolution since the  
128 Early Palaeozoic (Chen and Wilson, 1996; Dai, 2011; Jin et al., 2010; Yan et al., 2011).

129 The initial tectonic events were associated with the Palaeozoic Caledonian Orogeny  
130 caused by the closure of the Tethys ocean, with thrusting causing numerous  
131 unconformities between the Early Palaeozoic strata (Jin et al., 2010). Following the  
132 Caledonian Orogeny (Early Devonian), the Longmen Shan belt changed into a passive  
133 continental margin throughout the Devonian and Permian that was associated with  
134 extensional tectonism (Jia et al., 2006; Li et al., 2012; Tian, 2009; Zhou et al., 2013).

135 The most severe deformation recorded in the Longmen Shan thrust belt relates to the  
136 Late Triassic to Early Cretaceous NW to WNW directed under-thrusting of the South  
137 China block beneath the North China block (Chen and Wilson, 1996; Dai et al., 2009;  
138 Jin et al., 2010; Liu et al., 2005; Yan et al., 2011). These tectonic events resulted in  
139 structural unconformities within the Triassic and between the Upper Triassic and Lower  
140 Jurassic strata (Tian, 2009), numerous faults (e.g., Beichuan-Yingxiu Faults, Anxian-  
141 Dujiangyan Faults and the high angle reverse fault in this study (Fig. 3B)) (Arne et al.,  
142 1997; Chen et al., 1995; Wilson et al., 2006), intensive folding of the Jurassic strata and  
143 led to the uplift and erosion of Cretaceous strata (Li et al., 2008). The absolute timing of  
144 tectonism is constrained by Sensitive High Resolution Ion Microprobe analysis  
145 (SHRIMP) U–Th–Pb monazite, conventional U–Pb titanite, Sm–Nd garnet, and Rb–Sr  
146 muscovite and biotite ages on metamorphic rocks from the Danba Domal Metamorphic

147 Terrane ~100 km northwest of the southern sector of the Longmen Shan Thrust Belt.  
148 The available geochronology yield three age groups (ca. 200, ca. 160 and ca. 120 Ma)  
149 (Huang et al., 2003; Jin et al., 2010; Jin et al., 2008; Yan et al., 2011). Further age  
150 constraints for the timing of tectonism are given by  $^{40}\text{Ar}/^{39}\text{Ar}$  garnet and zircon fission  
151 track dates (ca. 110 - 130 Ma) from the middle district of the Longmen Shan Thrust Belt  
152 (Liu et al., 2001), and  $^{40}\text{Ar}/^{39}\text{Ar}$  muscovite and sericite dates (ca. 237 - 183 Ma) from  
153 the basement complex, detachment fault zone and ductile deformation zone from the  
154 northern part of the Longmen Shan Thrust Belt (Yan et al., 2011). The most recent  
155 tectonism recorded by the Longmen Shan Thrust Belt occurred during the Cenozoic as a  
156 result of the India-Asia continental collision (Dai, 2011; Li et al., 2008; Yan et al.,  
157 2011). This event further reactivated previous existing thrust faults and caused  
158 exhumation along the belt (Harrowfield and Wilson, 2005; Lei et al., 2012; Yan et al.,  
159 2011). Low-temperature thermochronology, such as apatite fission track (AFT) and (U-  
160 Th)/He methods, indicate a series of uplift events since the Late Cretaceous (Arne et al.,  
161 1997; Deng et al., 2012; Lei et al., 2012; Yan et al., 2011). Additionally, present day  
162 activity along the Longmen Shan Thrust Belt is evidenced by the 2008 Wenchuan  
163 earthquake (7.9  $M_w$  – epicentre in Wenchuan City) and the 2012 Ya'an earthquake (6.6  
164  $M_w$  – epicentre in Ya'an City) (Feng et al., 2014).

165 The northern segment of the Longmen Shan Thrust Belt, located to the north of Anxian  
166 County, extends for ~200 km (Fig. 1C). This segment of the belt contains several major  
167 thrust sheets and a blind frontal thrust zone, with most of the folds and thrust sheets  
168 emplaced towards the southeast (Jia et al., 2006; Jin et al., 2010; Jin et al., 2009a).  
169 Precambrian to Quaternary strata are present in the northern Longmen Shan Thrust Belt  
170 (Jia et al., 2006; Jin et al., 2009a). The Precambrian to Cambrian units mainly consist of

171 organic-rich black shales and siltstones with a total thickness of ~200 m (Rao et al.,  
172 2008; Wang et al., 2005; Xie et al., 2003). The Ordovician to Silurian units are largely  
173 absent due to uplift and erosion during the Caledonian Event (ca. 450 – 400 Ma) in the  
174 Yangtze Block. Devonian and/or Carboniferous strata, which mainly consist of dolomite  
175 and limestones, unconformably overlie the older units and possess a thickness ~50 –  
176 250 m. The Permian strata, which have a total thickness ~270 - 470 m, consist of  
177 limestone and black shales (Rao et al., 2008; Wang et al., 2005; Xie et al., 2003). The  
178 Early-Mid Triassic strata include ~750 m of limestones interbedded with sandstones or  
179 shales. The Late Triassic units of ~400 m thickness comprise interbedded sandstones  
180 and mudstones (Zhou et al., 2013). The overlying Jurassic and Cretaceous  
181 fluviolacustrine sediments comprise mudstones, sandstones and siltstones with a total  
182 thickness of up to 4500 m (Fig. 2).

183 The Upper Neoproterozoic to Lower Cambrian shales and middle Permian black  
184 mudstones are considered as the potential source rocks (Xie et al., 2003; Zhou et al.,  
185 2013) to several petroleum systems (e.g., Ningqiang, Tanjingshan and Kuangshanliang)  
186 in the northern Longmen Shan Thrust Belt (Chen et al., 1994; Huang and Wang, 2008;  
187 Tissot and Welte, 1984). Reservoir units include the Upper Cambrian, Lower Devonian,  
188 Lower and Upper Permian, Lower Triassic and Upper Jurassic carbonates, sandstones  
189 and/or siltstones (Chen and Wilson, 1996; Li et al., 1999; Worley and Wilson, 1996;  
190 Zhou et al., 2013). Devonian marine mudstones, Triassic gypsum, and Jurassic to  
191 Cretaceous mudstones act as seals to the several petroleum systems (Zhou et al., 2013)  
192 (Fig. 2).

193 The Kuangshanliang petroleum system is characterized by the largest and most  
194 complete anticline in the frontal thrust zone of the northern Longmen Shan Thrust Belt

195 (Fig. 3A) (Chen et al., 2005). The anticline comprises Cambrian strata in the core,  
196 surrounded by Ordovician to Triassic units (Fig. 3A). Bitumen and present day oil seeps  
197 in the Kuangshanliang anticline occur in the 565 m thick marine clastics of the Lower  
198 Cambrian Changjianggou Formation (Fig. 3A, B) as dykes or along faults and/or  
199 fractures that trend NW-SE. The calculated total hydrocarbon reserves in the  
200 Kuangshanliang anticline are ~70 Mbbl of oil (Tian, 2009).

201

### 202 3. Samples

203 Bitumen and oil seep samples were collected between 2010 and 2011 from field  
204 outcrops of bitumen dykes, fault planes, fault zones, fractures and seeps, in the  
205 Cambrian Changjianggou Formation (Figs. 3, 4). The densely forested nature of the area  
206 has resulted in there being no known outcrops of the bitumen dykes. The bitumen dykes  
207 were only accessible through old mine adits. Samples were obtained through three old  
208 mine adits approximately 8 km north of Shangsi, Jiange County (Fig. 3A). Access to  
209 these adits has been prohibited since 2012 for health and safety reasons. The dykes are  
210 ~0.5 - 10 m wide and occur over a known strike (NW) distance of ~50 m. The dykes  
211 typically run parallel to faults that show a dextral motion and dip ~35° towards the  
212 southwest. The contacts between the bitumen dykes and the country rock are sharp,  
213 although bitumen also impregnates the wallrocks up to ~10 cm from the edge of the  
214 dyke.

215 Two dykes (Dykes 1 and 2) are located within ~500 m of each other. Dyke 1 was  
216 accessed from the mine adit Shang Kuang Dong (upper bitumen hole). The dyke strikes  
217 NW over a distance of at least 100 m, and averages a width of 70 - 100 cm. The eastern  
218 contact with the Cambrian Changjianggou Formation sandstone is sharp, but the

219 western contact is brecciated (Fig. 4A). The breccia zone is ~10 cm wide and contains 1  
220 - 5 mm clasts of both the country rock (sandstone) and bitumen. Inward from the  
221 brecciated area, the western edge of Dyke 1 is intensively fractured over 10-20 cm.  
222 Three bitumen samples (11SKD-3d, 11SKD-4d and 11SKD-5d) were taken, ~2 m apart,  
223 from the centre of the dyke, which represents the least fractured part of Dyke 1 (Fig.  
224 4B). A fourth sample (SKD-1f) was taken from a cross-cutting bitumen-filled fracture  
225 (Fig. 4B). Dyke 2 was accessed from mine adit Xia Kuang Dong (lower bitumen hole).  
226 Two bitumen samples (XKD-1d; XKD-2d) were collected from the center of this dyke,  
227 ~5 m apart (Fig. 4C). Dyke 2 is narrower than Dyke 1 (20 - 50 cm), and strikes NW for  
228 at least 100 m. Both the western and eastern contacts with the host rock are sharp, with  
229 the adjacent country rocks being impregnated with bitumen up to 10 cm from the  
230 contact. In contrast to Dyke 1, the eastern margin of Dyke 2 is part of a low-angle  
231 reverse fault (Fig. 4C). The fault plane strikes NE and dips 34° to the NNW, with  
232 transport direction towards the SE. These fault characteristics are consistent with the  
233 overall pattern and geometry of thrusting in the northern Longmen Shan Thrust belt  
234 (Chen et al., 2005; Tian, 2009). The fault plane and associated gouge is confined to a 5  
235 cm thick, clay-rich siltstone interbed of the Cambrian Changjianggou Formation  
236 sandstone. The gouge has a sharp upper contact and diffuse basal contact. The bitumen  
237 impregnated into the sandstone country rock indicates a SE-ward fault motion syn-post  
238 emplacement of the bitumen Dyke 2 (Fig. 4D).

239 Seven additional bitumen samples (GY1d-6d and HSCD-1d) were collected from a third  
240 Dyke (Dyke 3) from the Huoshicun mine hole, ~2 km to the south of Dykes 1 and 2.  
241 Samples in Dyke 3 were collected along the centre of the main bitumen dyke body (Fig.  
242 4E). Dyke 3 has a similar strike orientation to that of Dykes 1 and 2 (NW), and

243 possesses a similar width to Dyke 2 (30 – 50 cm). Both the eastern and western dyke  
244 contacts are sharp, with little to no bitumen impregnated into the sandstone, and with no  
245 evidence of post-emplacement fracturing or faulting observed.

246 In the Northern Longmen Shan Thrust Belt, dextral strike-slip faults striking NE and  
247 dipping 30-40° NW are well developed (Burchfiel et al., 1995; Chen et al., 2005; Yan et  
248 al., 2011). In this study, the bitumen samples were also collected from two separate  
249 faults (Fig. 4F,G). Samples LXB-1f and LXB-2f were collected from the same fault,  
250 which strikes NE and dips 75° NW (Fig. 4F). The samples were taken ~2 m apart.  
251 Sample 11LXB-1f was collected from part of a slickenline striking NE with a dip of 45°  
252 NNW (Fig. 4G).

253 At the Huoshicun mine hole, oil was observed seeping through the Changjianggou  
254 Formation sandstone, three oil samples (Oil-3, Oil-5, Oil-7) were collected over a  
255 distance of 1 m (Fig. 4H).

256

#### 257 **4. Analytical Protocols**

258 The Gas Chromatography (GC) and Gas Chromatography-Mass Spectrometry (GC-MS)  
259 analyses on nine bitumen samples (GY-1, 3, 5, 11SKD-4, 11LXB-1, HSCD-1, SKD-1,  
260 XKD-1 and LXB-1) and two present day oil seep samples (Oil-3 and Oil-5) were  
261 conducted in Wuxi Institute of Petroleum Geology, Sinopec, China and Weatherford  
262 Laboratories, USA, following the analytical procedure of Hackley et al., 2013 . The  
263 bitumen samples were first cleaned with distilled water, to ensure there were no  
264 weathered contaminants on the surface, and then crushed to 100 mesh size using an  
265 agate pestle and mortar. Approximately 100 g of bitumen was put into a Soxhlet  
266 extractor for 72 hours to obtain the chloroform extract (asphalt). The asphalt was then

267 precipitated using *n*-hexane. For the oil samples, ~30 mg of crude oil sample was  
268 dissolved in 50 mL of *n*-hexane and left for 12 h at room temperature. The solution was  
269 then filtered, with all the filtrates collected and evaporated under nitrogen gas to 0.5 mL.  
270 A chromatographic column (30 cm × 10 mm in diameter) was prepared using a mixed  
271 stationary phase of activated silica gel and alumina at a ratio of 3:2 by referring to  
272 relevant literature (e.g., Yang et al., 2009). The concentrated sample was transferred to  
273 the chromatographic column for further separation. The saturated hydrocarbon fraction  
274 was eluted with *n*-hexane (25 mL). The fractions were then carefully concentrated under  
275 nitrogen flow to 0.5 mL for GC-MS analysis. The GC-MS system consisted of an  
276 Agilent 7890 GC, and an Agilent 5975C mass spectrometer. A DB-5MS column 50 m ×  
277 0.25 mm × 0.25 μm was used. High purity helium (99.9995%) was used as a carrier gas  
278 at a flow rate of 1.0 mL/min. The injector temperature was 300°C. The injection volume  
279 was 1.0 L. All injections were done with a 7683B series autosampler. The oven  
280 temperature was programmed from 50°C (1 min hold) to 100°C at 10°C /min, and then  
281 to 310°C (20 min hold) at 2°C /min. The mass spectrometer was operated in the electron  
282 impact mode (70 eV). The temperature of ion source and transfer-line were set at 230°C  
283 and 300°C, respectively. The scanned mass range was from 50 to 550 u. The  
284 temperature of the Quadrupole was held at 150°C.

285 For Re-Os analysis, approximately ~0.2 - 1.0 g bitumen was separated from the 16  
286 samples. All samples were isolated without metal contact and handpicked. Samples  
287 were crushed to ~1 mm grains using an agate pestle and mortar. For the oil seeps, the  
288 asphaltene fraction was analyzed as Re and Os are predominantly contained within the  
289 asphaltene fraction of oil (Selby et al., 2007). The asphaltenes were precipitated from  
290 the oil using 40 times volume of *n*-heptane (~1 g oil with 40 ml solvent) at room

291 temperature for at least 8 hrs. The asphaltene abundance of the present day oil seeps are  
292 between 9.48 and 13.54 % (Table 1). The Re and Os isotopic compositions, and  
293 abundances of the bitumen and asphaltene from the oil were analysed at the Laboratory  
294 for Source Rock and Sulfide Geochronology and Geochemistry (a member of the  
295 Durham Geochemistry Centre) at Durham University following published analytical  
296 procedures (e.g. Selby et al., 2005; Selby et al., 2007). Approximately 100 - 200 mg of  
297 bitumen or asphaltene were dissolved and equilibrated with a known amount of  $^{185}\text{Re}$   
298 and  $^{190}\text{Os}$  spike solution by inverse *aqua-regia* (3 ml HCl and 6 ml  $\text{HNO}_3$ ) in a Carius  
299 tube for 24 hours at 220°C. Osmium was isolated and purified from the inverse *aqua-*  
300 *regia* by  $\text{CHCl}_3$  solvent extraction at room temperature and micro-distillation. The Re  
301 was isolated using HCl- $\text{HNO}_3$  based anion chromatography. The purified Re and Os  
302 were loaded on Ni and Pt filaments and analyzed using Negative Ion Thermal Ionization  
303 Mass Spectrometry (N-TIMS). Measured Re and Os ratios were corrected for mass  
304 fractionation using  $^{185}\text{Re}/^{187}\text{Re} = 0.59738$  (Gramlich et al., 1973) and  $^{192}\text{Os}/^{188}\text{Os} =$   
305 3.08261, spike and blank contributions. All data were blank corrected based on the total  
306 procedural blanks values of Re ( $1.6 \pm 0.025$  pg) and Os ( $0.05 \pm 0.004$  pg), with an  
307 average  $^{187}\text{Os}/^{188}\text{Os}$  ratio of  $\sim 0.22 \pm 0.06$  (n = 4). All uncertainties include the  
308 propagated uncertainty in the standard, spike calibrations, mass spectrometry  
309 measurements, and blanks. In-house Re (Restd) and Os (AB2) solutions were analyzed  
310 as a monitor of reproducibility of isotope measurements. The analyses presented in this  
311 study were conducted prior to using DROsS as our in-house control solution (Nowell et  
312 al., 2008). The  $^{187}\text{Os}/^{188}\text{Os}$  values of the Os standard solution AB2 during this study  
313 were  $0.1611 \pm 0.0066$ , with the  $^{185}\text{Re}/^{187}\text{Re}$  values of the Re standard solution being  
314  $0.5984 \pm 0.0002$ . These values are in agreement with those previously published for



315 AB2 and Restd (Cumming et al., 2014; Finlay et al., 2011, 2012; Lillis and Selby, 2013;  
316 Rooney, 2011). The  $^{185}\text{Re}/^{187}\text{Re}$  ratios for samples of this study were corrected for the  
317 measured difference of the  $^{185}\text{Re}/^{187}\text{Re}$  value for Restd and the  $^{185}\text{Re}/^{187}\text{Re}$  value of  
318  $0.59738 \pm 0.00039$  (Gramlich et al., 1973). The Re–Os data of this study are regressed  
319 using the program *Isoplot* V. 4.15 (Ludwig, 2003) with  $^{187}\text{Re}$  decay constant of  
320  $1.666 \times 10^{-11} \text{a}^{-1}$  (Smoliar et al., 1996). The input data contains  $^{187}\text{Re}/^{188}\text{Os}$  and  $^{187}\text{Os}/^{188}\text{Os}$   
321 ratios with their total  $2\sigma$  uncertainty and associated error correlation, Rho.

322

## 323 **5. Results**

324 This study presents results of organic geochemistry for nine bitumen and two present  
325 day oil seeps, and Re–Os data for the sixteen bitumen samples and three present day oil  
326 seeps. The detailed results of the organic geochemistry and Re–Os analysis are presented  
327 below.

328

### 329 **5.1 GC-MS results**

330 Nine samples from the three bitumen dykes and bitumen from faults/fractures were  
331 selected for detailed organic geochemistry analysis (Table 1). Component analysis show  
332 that the asphaltene fraction occupies more than 98 % of the total bitumen sample (Table  
333 1). The saturate fraction gas chromatograms (SFGCs) of the analyzed bitumen samples  
334 are dominated by humps of unresolved compounds (UCM) with some discrete peaks  
335 superimposed (Fig. 5). The UCM exhibited by the SFGCs indicates that the samples  
336 have been extensively biodegraded with compounds, such as *n*-alkanes and acyclic  
337 isoprenoids, removed by microbial action. This is also supported by the presence of  
338 Nor-25-hopane (Wenger and Isaksen, 2002) (Fig. 5). Gas chromatograms show that the

339 Carbon Preference Index (CPI) value based on the formula  $(NC_{23}+NC_{25}+NC_{27})+$   
340  $(NC_{25}+NC_{27}+NC_{29})/(2*(NC_{24}+NC_{26}+NC_{28}))$  ranges from 0.35 to 2.59, with  
341 majority of samples possessing CPI values between ~0.91 and 1.21 (except LXB-1f and  
342 HSCD-1d). The calculated Pr/Ph ratio for samples 11SKD-4d (Dyke 1), XKD-1d (Dyke  
343 2) and HSCD-1d (Dyke 3) range from 0.47 to 0.95. The bitumen samples show peak  
344 values for tricyclic terpanes ( $C_{19}$  to  $C_{30}$ ) at  $C_{21}$  or  $C_{23}$  (Fig. 5). The  $C_{23}/C_{21}$  tricyclic  
345 terpane values range from 0.89 to 1.67, with an average of 1.35. The  $C_{24}$  tetracyclic/ $C_{26}$   
346 tricyclic terpane ratios range from 1.00 to 2.61, with only two samples (11SKD-4 and  
347 SKD-1) possessing ratios  $>2.0$  (Table 1). The hopanes ( $C_{27}$  to  $C_{35}$ ) exhibit peaks at  $C_{29}$   
348 or  $C_{30}$  (Fig. 5). The abundance of the  $C_{31}$  to  $C_{35}$  hopanes decrease with increasing carbon  
349 number. In addition to the presence of  $C_{30}$  diahopane, Ts ( $18\alpha(H)$ -trisorhopane), and  
350 Tm ( $17\alpha(H)$ -trisorhopane), and gammacerane are also detected (Fig. 5). The  
351  $Ts/(Ts+Tm)$  values range from 0.20 to 0.38, with an average of 0.31,  $DH_{30}/H_{30}$  values  
352 range from 0.02 to 0.08, with an average of 0.05, and  $C_{32}$  hopane S/(S+R) values range  
353 from 0.54 to 0.62, with an average of 0.58. The bitumen samples yield a gammacerane  
354 index of 0.12 to 0.22, with an average of 0.16. The ratio of Nor-25-hopane/hopane  
355 range from 0.07 to 0.19, with the exception of sample SKD-1f, which has a ratio of  
356 0.07, all other samples possess a similar ratio (0.15).

357 Sterane compounds including  $C_{21}$  pregnane,  $C_{22}$  sterane, diasterane and  $C_{27}$ - $C_{29}$  sterane  
358 were also detected (Fig. 5). The ratio of  $S_{21}/S_{22}$  range from 2.36 to 2.58, with an average  
359 of 2.44.  $C_{27}$ ,  $C_{28}$ ,  $C_{29}$  steranes of all the bitumen display a similar V-shape distribution  
360 which occupy ~30.2, 16.0 and 53.8 %, respectively, with  $C_{29}$  sterane exhibiting the  
361 highest abundance. The ratio of  $C_{29}\alpha\alpha\alpha 20S/(20S+20R)$  and  $C_{29}\beta\beta/(\beta\beta+\alpha\alpha)$  vary from  
362 0.46 to 0.52 and 0.49 to 0.57, respectively, which yield a similar Ro value (~0.9). The

363 organic geochemistry of the bitumen samples analyzed in this study suggest that all the  
364 bitumen has middle to high maturity, and was sourced from similar organic matter  
365 derived from marine algae deposited in an anoxic environment (De Grande et al., 1993;  
366 Didyk, 1978; Peters et al., 2005; Seifert and Moldowan, 1986).

367 However, the organic analysis of two of the present day oil seep samples (Oil-3 and  
368 Oil-5) show very different organo-geochemical features as compared to the bitumen.  
369 This observation is critical given that these samples are taken in close spatial (~20 m)  
370 proximity to the bitumen samples GY-6 and HSCD-1, which suggests that the organo-  
371 geochemical characteristics of the bitumen have not been appreciably affected by the  
372 present oil seeps. The SFGCs display UCM and suggest severe biodegradation of the  
373 present day oil seeps (Fig. 5). Given the lack of the majority of the *n*-alkanes, the data  
374 related to CPI or Pr/Ph values can not be calculated. Terpanes and hopanes, except for  
375 the Ts/(Ts+Tm) ratio (0.31 vs 0.36), of the oil are similar to the bitumen. Further, all of  
376 the other parameters, for example gammacerane/hopane (3.91-7.59), C<sub>24</sub> tetracyclic/C<sub>26</sub>  
377 tricyclics (0.51-0.52) and DH<sub>30</sub>/H<sub>30</sub> (3.10-5.54) values are distinctly different in  
378 comparison to the bitumen samples (Table 1). Only C<sub>21</sub> and C<sub>22</sub> steranes in the oil were  
379 detected, which yield a S<sub>21</sub>/S<sub>22</sub> ratio of 0.21 and 0.20, respectively, which are also  
380 different as compared to the bitumen. The limited organic data for the present day oil  
381 seep samples suggests that the organic fraction of the oil is derived from a source rock  
382 deposited in a hypersaline, suboxic and clay-rich environment (Peters and Moldowan,  
383 1993; Zumberge, 1987).

384

## 385 5.2 Re-Os results

386 The Re and Os abundances of all the bitumen samples range between 283.1 and 547.9

387 ppb, and 4.06 and 15.3 ppb, respectively (Table 2). These values are significantly  
388 elevated from those of the average continental crust (Esser and Turekian, 1993), but  
389 similar to previously reported bitumen samples, and the organic-rich sedimentary rocks  
390 (Cohen et al., 1999; Esser and Turekian, 1993; Georgiev et al., 2016; Ravizza and  
391 Turekian, 1992; Rooney et al., 2010; Selby and Creaser, 2005; Xu et al., 2009; Xu et al.,  
392 2014). The  $^{187}\text{Re}/^{188}\text{Os}$  values of the bitumen range from 229.5 to 595.1 and exhibit a  
393 radiogenic  $^{187}\text{Os}/^{188}\text{Os}$  composition of 2.79 to 3.56 (Table 2). Repeat analyses of a  
394 single bitumen sample (11SKD-4d-rpt) yield highly reproducible (<1%) Re ( $\sim 512.2 \pm$   
395  $1.8$  vs  $518.8 \pm 1.3$  ppb) and Os ( $14478.3 \pm 46.3$  vs  $14605.3 \pm 75.8$  ppt) concentrations,  
396 and  $^{187}\text{Re}/^{188}\text{Os}$  ( $230.7 \pm 0.9$  vs  $231.5 \pm 1.0$ ) and  $^{187}\text{Os}/^{188}\text{Os}$  ( $2.84 \pm 0.01$  vs  $2.83 \pm 0.01$ )  
397 values (Table 2). Similar reproducibility has been shown by previous studies (Lillis and  
398 Selby, 2013; Selby et al., 2005).

399 Collectively the bitumen Re-Os isotope data from the three dykes, fault and fracture  
400 surfaces does not show any linear relationship, and shows a large range in isotope  
401 compositions (Fig. 6A). Herein we discuss the Re-Os data of each bitumen occurrence  
402 separately. The three samples from Dyke 1 have extremely similar Re-Os isotope  
403 compositions, and as a result do not yield a meaningful Re-Os date ( $674 \pm 490$  Ma).  
404 Bitumen from a fracture (SKD-1f) that postdates Dyke 1 exhibits broadly similar  
405  $^{187}\text{Os}/^{188}\text{Os}$ , but higher  $^{187}\text{Re}/^{188}\text{Os}$  values than that of the dyke (Table 2). The two  
406 bitumen samples from Dyke 2 show distinctly different Re-Os isotope compositions in  
407 comparison to Dyke 1, specifically with respect to the  $^{187}\text{Re}/^{188}\text{Os}$  values. Although,  
408 dates derived from only two samples may not be completely reliable geologically, the  
409 Re-Os data from the two Dyke 2 bitumen samples may suggest that bitumen formation  
410 occurred during the Early Jurassic ( $181 \pm 41$  Ma). Bitumen from Dyke 3 exhibit the

411 largest variation in Re-Os isotope space, with the compositions specifically different to  
412 Dyke 1 (with the exception of GY-5d) and Dyke 2. The Re-Os data of Dyke 3 yield a  
413 Model 3 (which assumes that the scatter in the degree of fit of the data is a combination  
414 of the assigned uncertainties, plus a normally distributed variation in the  $^{187}\text{Os}/^{188}\text{Os}$   
415 values (Ludwig, 2003)) date of  $503 \pm 140$  Ma (Mean Squared Weighted Deviation,  
416 MSWD = 90), with an initial  $^{187}\text{Os}/^{188}\text{Os}$  value of  $0.91 \pm 0.71$  (Fig. 6B). The Re-Os date  
417 and its uncertainty is largely controlled by sample GY-5d that controls the lower anchor  
418 of the best-fit line of the data, and HSCD-1 and GY-1d which plot above the best-fit  
419 line, respectively. Using the Re-Os date of 503 Ma to calculate the initial  $^{187}\text{Os}/^{188}\text{Os}$   
420 ( $\text{Os}_i$ ) values, shows that samples HSCD-1 and GY-1d possess  $\text{Os}_i$  values ( $\sim 1.0$ ) that are  
421 slightly more radiogenic than the samples GY-2d, 3d, 4d, 5d, and 6d (0.85 - 0.89), and  
422 we consider that the samples HSCD-1 and GY-1d are the principal controls on the Re-  
423 Os date and uncertainty (Table 2). Considering only the samples (GY-2d, 3d, 4d, 5d,  
424 and 6d) that possess similar  $\text{Os}_i$  values, the Re-Os data yield a more precise Re-Os date  
425 of  $483 \pm 27$  Ma, with an  $\text{Os}_i$  value of  $0.97 \pm 0.13$ .

426 The Re-Os isotope data of bitumen sampled from faults and fractures show no linear  
427 trends. Sample 11LXB-1f possesses similar  $^{187}\text{Re}/^{188}\text{Os}$  and  $^{187}\text{Os}/^{188}\text{Os}$  values to those  
428 of Dyke 3, specifically GY-3d and 4d. In contrast, the Re-Os data of SKD-1f, LXB-1f  
429 and 2f are similar to that for Dyke 2. Combined, the bitumen Re-Os data of Dyke 2 and  
430 from the fractures represented by samples SKD-1f, LXB-1f and 2f define a broadly  
431 positive correlation between the  $^{187}\text{Re}/^{188}\text{Os}$  and  $^{187}\text{Os}/^{188}\text{Os}$  compositions, and yield a  
432 Re-Os date of  $158 \pm 76$  Ma, with an  $\text{Os}_i$  value of  $1.85 \pm 0.61$  (MSWD = 79) (Fig. 6E).  
433 The uncertainty in this date is because samples (LXB-1f, SKD-1f, LXB-2f, XKD-2d)  
434 though very close to the linear regression, still deviate from the line of best-fit. The  $\text{Os}_i$

435 values calculated at 158 Ma show that samples LXB-1f and SKD-1f possess less  
436 radiogenic  $Os_i$  values (1.80 and 1.75) in comparison to XKD-1d, XKD-2d and LXB-2f  
437 (1.87 to 1.91) (Table 2). Treated separately the Re-Os data for samples XKD-1d, XKD-  
438 2d and LXB-2f, and samples LXB-1f and SKD-1f record a Mid Jurassic age ( $162 \pm 14$   
439 Ma, with an  $Os_i$  value of  $1.87 \pm 0.12$ , and  $172.6 \pm 8.1$  Ma, with an  $Os_i$  value of  $1.66 \pm$   
440  $0.06$ , respectively) (Fig. 6F).

441 The present day oil seep samples possess very different Re-Os systematics as compared  
442 to all the bitumen samples. In contrast to the bitumen samples the asphaltene fractions  
443 of the oil seep samples possess much lower Re and Os abundances (Re of 7.7 to 9.6 ppb,  
444 Os of 90.3 to 127.2 ppt) (Table 2). The  $^{187}Re/^{188}Os$  and  $^{187}Os/^{188}Os$  values of the oils are  
445 very similar, 496.3 to 579.3 and 2.89 to 2.93, respectively (Table 2). As the three oil  
446 seep samples possess very similar Re and Os isotope compositions, no meaningful Re-  
447 Os date can be determined.

448

## 449 **6. Discussion**

### 450 **6.1 Bitumen and Oil Geochemistry and source tracing**

451 In this study, the biomarker analysis shows that all the bitumen from the dykes,  
452 fractures and faults possess similar organo-geochemical characteristics, distinct from the  
453 present day oil seeps. The bitumen molecular composition (*n*-alkanes, terpanes and  
454 steranes) are interpreted to suggest that the bitumen organic matter derived from a  
455 marine source deposited in an anoxic setting, are mature ( $R_o$ :  $\sim 0.8 - 1.0$ ) and  
456 biodegraded (Pr/Ph ratio = 0.47-0.95; Gammacerane/H30 =  $\sim 0.16$ ;  $C_{23}/C_{21}$  tricyclic =  
457  $\sim 1.35$ ;  $C_{24}$  tetracyclic /  $C_{26}$  tricyclics =  $\sim 1.41$ ;  $Ts/(Ts+Tm)$  =  $\sim 0.31$ ; diahopane/hopane  
458 =  $\sim 0.05$  and  $H_{32} S/(R+S)$  homohopane =  $\sim 0.58$ ; the 25-nor-hopane/hopane =  $\sim 0.15$ )

459 (Table 1) (Peters and Moldowan, 1993; Wenger and Isaksen, 2002; Zumberge, 1987).  
460 Further, the sterane chromatogram ( $m/z = 217$ ), pregnane/homopregnane ratio ( $\sim 2.44$ ),  
461 as well as the V-shape  $C_{27}$ - $C_{29}$  sterane distribution, with  $C_{29}$  being the largest  
462 component, implies that all the bitumen in the study area is derived from the same  
463 source rock (e.g. Peters and Moldowan, 1993; Wu et al., 2012). The  $C_{29}$   $\alpha\alpha$  S/(S+R)  
464 and  $C_{29}$   $\beta\beta$ /( $\beta\beta$ + $\alpha\alpha$ ) ratios (0.49 and 0.53, respectively) also indicate that the bitumen  
465 was generated during peak oil generation (Georgiev et al., 2016; Peters and Moldowan,  
466 1993).

467 In comparison to the bitumen samples the present day oil samples are severely  
468 biodegraded and are slightly less mature ( $T_s/T_{s+T_m}$  ratio = 0.36) (Table 1; Fig. 5). The  
469 remaining biomarker parameters ( $\text{gammacerane/hopane} = 7.59$  and  $3.91$ ;  $C_{24}$   
470  $\text{tetracyclic}/C_{26}$   $\text{tricyclics} = 0.52$ ;  $\text{diahopane/hopane} = 5.54$  and  $3.10$ ;  $\text{pregnane}/$   
471  $\text{homopregnane} = 0.21$ ) are supportive of the organo-geochemical signature of the  
472 present day oil seeps being derived from the organic matter deposited in a sub-oxic  
473 marine-continental sedimentary environment (Peters and Moldowan, 1993; Zumberge,  
474 1987). The Late Neoproterozoic to Early Cambrian Doushantuo and Qiongzhusi  
475 formations and the Upper Permian Dalong Formation are considered to be the principal  
476 source rocks in the Kuangshanliang area (Huang et al., 2011; Lin et al., 2011; Liu et al.,  
477 2009; Sun et al., 2009; Wei et al., 2008). Previous work shows that the geochemical  
478 parameters of both  $C_{23}$   $\text{tricyclics}/C_{24}$   $\text{tetracyclic}$  and  $\text{pregnane}/\text{homopregnane}$  are  
479 higher ( $>2.5$  and  $\sim 2.0$ ) for the Late Neoproterozoic-Early Cambrian formations than for  
480 the Upper Permian Dalong Formation ( $<1.6$  and  $\sim 1.0$ ) (Wu et al., 2012). In this work,  
481 the  $C_{23}$   $\text{tricyclics}/C_{24}$   $\text{tetracyclic}$  and  $\text{pregnane}/\text{homopregnane}$  ratio of the bitumen  
482 samples are respectively  $\sim 2.42$  and  $\sim 2.44$ , however, for the present day oil seep samples,

483 these organic parameter ratios are only ~0.25 and 0.20 (the ca. 5 times lower ratio  
484 compared with Permian mudstone may be caused by the biodegradation of the present  
485 day oil seeps). Given that hydrocarbons possess similar biomarker characteristics to that  
486 of its source unit (Cole et al., 1987; Pusey, 1973; Wu et al., 2012; Zhang et al., 2000),  
487 the results of this study suggest that the bitumen and oil seeps are sourced from different  
488 units, with the bitumen being sourced predominantly from the shales of the Late  
489 Neoproterozoic Doushantuo and Early Cambrian Qiongzhusi formations, and the  
490 present day oil seeps from the mudstones of the Permian Dalong Formation. The  
491 identification of the Doushantuo and Qiongzhusi formations being the source of the  
492 bitumen in the Kuangshanliang area further supports the oil-source correlation based on  
493 the similar  $\delta^{13}\text{C}$  values for bitumen and the Doushantuo and Qiongzhusi formations  
494 (bitumen = -35.71 ‰ to -27‰ (Wu et al., 2012; Zhou et al., 2013); Precambrian-  
495 Cambrian = -30.3‰ to -35.4‰; (Wu et al., 2012; Zhou et al., 2013)), in contrast to the  
496 oil and Dalong Formation (oil = -25.9‰ to -27.7‰ (Wu et al., 2012); Permian Dalong  
497 Formation = -25.9‰ to -27.7‰ (Liang, 2007; Zhou et al., 2013)).

498

## 499 **6.2 Multiple phases of petroleum generation**

500 Previous studies suggest that oil generation in the North Longmen Shan Thrust Belt and  
501 the adjacent Sichuan Basin is a result of the hydrocarbon maturation of the Late  
502 Neoproterozoic - Early Cambrian shales (e.g., Late Neoproterozoic Doushantuo and  
503 Early Cambrian Qiongzhusi formations) during the Middle Ordovician (Zhou et al.,  
504 2013; Zou et al., 2014b). The only Re-Os dataset that provides a robust estimation of oil  
505 generation during the Ordovician is the bitumen from Dyke 3. As discussed above, all  
506 the Re-Os bitumen from Dyke 3 yield a Model 3 date of  $503 \pm 140$  Ma (Fig. 6B).



507 However, considering only the Re-Os bitumen data of Dyke 3 that possess similar  $Os_i$   
508 values (GY-2d, 3d, 4d, 5d, and 6d;  $Os_i = 0.85 - 0.89$ ) calculated at 503 Ma, a Re-Os date  
509 of  $483 \pm 10$  Ma is determined. The absolute reason why the samples HSCD-1 and GY-  
510 1d possess slightly elevated  $Os_i$  values ( $\sim 1.0$ ) in comparison to the majority of the  
511 bitumen from Dyke 3 is not known. But the reasoning could be related slight post-  
512 depositional disturbance to the Re-Os systematics and/or continuous hydrocarbon  
513 generation. Both determined Re-Os ages are in agreement within uncertainty, with the  
514 more precise age determined, by the bulk of the sample set, providing an age that agrees  
515 well with modeling for the timing of burial ( $\sim 2500$  m and  $\sim 100$  °C) and source rock  
516 maturation of the Doushantuo and Qiongzhusi formations in the Northern Longmen  
517 Shan Thrust Belt and adjacent Sichuan Basin (Liu et al., 2009; Yuan et al., 2012; Zhou  
518 et al., 2013).

519 In contrast to Dyke 3, the bitumen Re-Os data from Dyke 1 yield no meaningful age  
520 because of the limited spread in  $^{187}Re/^{188}Os$  and  $^{187}Os/^{188}Os$  values. However, the  
521 bitumen Re-Os isotope compositions of Dyke 1 are similar to that of sample GY-5d  
522 from Dyke 3 (Table 2). Calculated at the age of Dyke 3 (483 Ma), the Re-Os bitumen  
523 data of Dyke 1 yield  $Os_i$  values (0.96-0.99) which is similar to the range of that  
524 determined for Dyke 3 (0.96 - 0.98; except GY-1 and HSCD-1) (Table 2). Based on the  
525 similarity of the GC-MS (e.g., m/z 191 and 217; Fig. 5) and Re-Os data of bitumen from  
526 the Dyke 1 and Dyke 3, we consider the bitumen to be of the same oil generation  
527 episode. Together, the Re-Os data from both Dyke 3 (except GY-1 and HSCD-1) and  
528 Dyke 1 yield a Model 3 date of  $486 \pm 15$  Ma (Fig. 6D).

529 In comparison to the bitumen from Dyke 1 and 3, the Re-Os characteristics of the five  
530 bitumen samples from Dyke 2 and faults/fractures have very different Re-Os

531 systematics. Calculated at 486 Ma the Re-Os data of Dyke 2 and faults/fractures yield  
532 negative  $^{187}\text{Os}/^{188}\text{Os}$  values (-0.05 to -1.04; [Table 2](#)). Furthermore, relative to a ca.486  
533 Ma reference isochron, the five samples of Dyke 2 and faults/fractures have higher  
534  $^{187}\text{Re}/^{188}\text{Os}$  ratios for a given  $^{187}\text{Os}/^{188}\text{Os}$  ([Fig. 6E](#)). This suggests that these bitumen  
535 samples are either of a different generation age to that of Dyke 1 and 3, or the Re-Os  
536 bitumen systematics of the Dyke 2 and faults/fractures have been disturbed.

537 The Re-Os data of the five bitumen samples from Dyke 2 (XKD-1d, XKD-2d) and  
538 fault/fractures (SKD-1f, LXB-1f, LXB-2f) together yield a Model 3 Re-Os date of 158  
539  $\pm 76$  Ma ( $^{187}\text{Os}/^{188}\text{Os} = 1.85 \pm 0.61$ , MSWD = 79) ([Fig. 6E](#)). For the Re-Os isotope  
540 compositions (e.g.,  $^{187}\text{Re}/^{188}\text{Os}$  and  $^{187}\text{Os}/^{188}\text{Os}$ ) to yield a statistically meaningful  
541 isochron date, the samples comprising the dataset must have formed contemporaneously,  
542 must possess the same initial ( $^{187}\text{Os}/^{188}\text{Os}$ ) isotope ratio, and the isotope systematics  
543 must not have been affected post formation ([Cohen et al., 1999](#); [Kendall et al., 2009](#);  
544 [Selby et al., 2007](#)). For these five bitumen samples, the degree of scatter about the best-  
545 fit line of the data, as given by the MSWD, is 76. The high MSWD indicates that one of  
546 the criteria for developing a statistically meaningful isochron has not been met.

547 Although post-depositional effects, different sample localities, and contemporaneity  
548 between the sample set may affect the Re-Os data, the positive correlation of the Re-Os  
549 data may indicate that the major reason for the scatter could be a result of variable initial  
550  $^{187}\text{Os}/^{188}\text{Os}$  values. Using the Re-Os date derived by the isochron (158 Ma), initial  
551  $^{187}\text{Os}/^{188}\text{Os}$  values ( $\text{Os}_i$ ) yield two populations for the sample set: (1) three samples with  
552  $\text{Os}_i$  values of  $\sim 1.89$  (samples XKD-1d, XKD-2d, LXB-2f); and (2) two samples with  
553  $\text{Os}_i$  values of  $\sim 1.77$  (samples SKD-1f; LXB-1f) ([Table 2](#)). Considering the sample set as  
554 two distinct populations, the three bitumen samples (XKD-1d, XKD-2d, LXB-2f) yield

555 a Model 1 Re-Os date of  $162 \pm 14$  Ma ( $Os_i = 1.87 \pm 0.12$ ; MSWD = 0.95; Fig. 6F).  
556 Although only two samples, the Re-Os data for bitumen samples SKD-1f and LXB-1f  
557 define Re-Os date of  $172.7 \pm 8.1$  Ma (Fig. 6F). Both the Re-Os dates are within  
558 uncertainty and suggest that these five bitumen formed broadly contemporaneously  
559 during the Middle Jurassic at 162 - 173 Ma.

560 The  $^{187}Os/^{188}Os$  composition of an hydrocarbon at its time of generation is inherited  
561 from its source (Finlay et al., 2011; Lillis and Selby, 2013; Selby and Creaser, 2005;  
562 Selby et al., 2005; Selby et al., 2007). The difference in the initial  $^{187}Os/^{188}Os$   
563 compositions of the two temporally distinct bitumen samples ( $\sim 0.95$  vs  $\sim 1.85$ ; Fig. 6;  
564 Table 2) could indicate the bitumen could have been derived from different source rocks.  
565 However, the organic geochemistry for all the bitumen samples are indicative of the  
566 source rock being the Late Neoproterozoic to Early Cambrian Doushantuo and  
567 Qiongzhusi formations. As such, the more radiogenic initial  $^{187}Os/^{188}Os$  compositions of  
568 bitumen formed during the Jurassic ( $\sim 1.85$ ) is the result of the greater duration of  
569 radioactive ingrowth of  $^{187}Os$  from the decay of  $^{187}Re$  in the source rock since its  
570 deposition. Although no Re-Os data was obtained for the potential source rock samples  
571 in this study, Re-Os data of the Late Neoproterozoic – Early Cambrian shales from the  
572 South China Block (Yangtze Gorges area (Kendall et al., 2009) and Zunyi, Guizhou  
573 province (Jiang et al., 2007)) yield  $Os_i$  values at ca. 485 Ma and ca. 165 Ma of 0.89 -  
574 0.98 and 1.54 - 2.01, respectively. The bitumen  $Os_i$  values at ca. 486 Ma and ca. 165 Ma  
575 in this study all fall into this range, which further supports the bitumen are derived from  
576 the same source, but during two separate phases of oil generation.

577 The Longmen Shan Thrust Belt records a series of complex tectonic events since the  
578 Palaeozoic (Chen and Wilson, 1996; Dai, 2011; Jin et al., 2010; Yan et al., 2011). Burial

579 history models (Zhou et al., 2013; Zou et al., 2014b) coupled with the Re-Os dates of  
580 the Dykes 1 and 3 suggest that oil generation of the Late Neoproterozoic Doushantuo  
581 and Early Cambrian Qiongzhusi formations in the Northern Longmen Shan Thrust Belt  
582 and the adjacent Sichuan Basin occurred during the Middle Ordovician. Oil generation  
583 ceased during the Caledonian Orogeny (~450 – 400 Ma) due to more than 2000 m of  
584 uplift and denudation (Wang et al., 1989; Wang et al., 2007; Zhuang, 1985; Zou et al.,  
585 2014b). The maturation history of the Early Cambrian Qiongzhusi Formation based on  
586 five different wells across the southwest Sichuan Basin indicates that the shales did not  
587 enter the oil window between the Late Devonian and Carboniferous (Liu et al., 2009).  
588 However, since Triassic, the Northern Longmen Shan Thrust Belt has been affected by  
589 the Indosinian–Yanshan orogenies following the collision between the North and South  
590 China blocks (Liu et al., 2005). Compressional tectonics in the Longmen Shan Thrust  
591 Belt and Sichuan Basin continued into the Late Jurassic from the paleogeography model  
592 (Jin et al., 2009b; Liu et al., 1996); apatite fission track date of  $162 \pm 23$  Ma (Arne et al.,  
593 1997); and post-tectonic granitoid magmatism at ~160 Ma (Jin et al., 2008) (Fig. 7). The  
594 sheared bitumen accumulations observed in the sandstone country rock (Fig. 4D) also  
595 suggests that the bitumen emplacement of Dyke 2 may be syn-tectonic. The Re-Os dates  
596 (ca.162 - 172 Ma) of the five bitumen samples from Dyke 2 and fault/fractures coincide  
597 with the timing of the tectonism in the Longmen Shan Thrust Belt during the Jurassic.  
598 The organic geochemistry of the Dyke 2 and fault/fracture bitumen suggest that it is  
599 sourced from the Late Neoproterozoic – Early Cambrian Doushantuo and Cambrian  
600 Qiongzhusi formations. These units were buried to more than 5000 m and re-entered the  
601 oil window ( $R_o \sim 1.2$  %) during the Middle Jurassic (Liu et al., 2009; Zou et al., 2014b).  
602 The hydrocarbon generation intensity of the Cambrian source rock units from the

603 Yangtze block (China) indicates that the Triassic and Middle Jurassic were the two peak  
604 oil generation intervals (Liang, 2007). Further, analysis on the Zi 1 and Gaoke 1 Wells  
605 from the center of the Sichuan Basin found that the Lower Cambrian shales achieved  
606 peak oil generation during the Middle Jurassic (ca. 175 – 161 Ma) (Liu et al., 2009;  
607 Zhang et al., 2005). Fluid inclusion homogenization temperatures (~120 °C) and basin  
608 modeling in the Weiyuan gas field in the southwest Sichuan Basin also indicate that oil  
609 generation and migration occurred during the Triassic and Jurassic (ca. 200 – 170 Ma)  
610 (Fig. 7) (Ma et al., 2007a; Tang et al., 2004; Zou et al., 2014b).

611 Integrating previous research work and the organic geochemistry, and Re-Os isotope  
612 analysis results of this study, we propose that the hydrocarbon evolution in  
613 Kuangshangliang area happened as follows:

614 (1) During the Early Palaeozoic, the Late Neoproterozoic Doushantuo and Early  
615 Cambrian Qiongzhusi formations were buried to a depth of more than 2500 m and  
616 entering the oil window ( $R_o \sim 0.80$ ), and leading to the first phase of oil generation.  
617 Following this oil generation event, the Caledonian Orogeny (~450 - 400 Ma) resulted  
618 in ~2000 m of uplift and thus halted hydrocarbon maturation of the Late Neoproterozoic  
619 and Early Cambrian source rocks (Fig. 7A, B).

620 (2) As a result of the collision following the Indosinian-Yanshan orogenies during the  
621 Triassic and Jurassic, the Late Neoproterozoic Doushantuo and Early Cambrian  
622 Qiongzhusi formations were buried to a depth of more than 5000 m ( $R_o \sim 1.2$ ) (Fig. 7C),  
623 leading to the second phase of oil generation from these formations.

624 (3) Although no meaningful Re-Os age can be obtained from the present day oil seeps,  
625 the organic geochemistry data generated in this study along with the previous research  
626 work indicates that this oil may have been generated during the Mesozoic from a

627 Permian source, i.e. the Dalong Formation (Fig. 7C).

628 (4) Since the Cretaceous, continued tectonics, due to the collision between the Indian  
629 and Asian plates, has caused the rapid uplift and denudation of the entire Longmen Shan  
630 Thrust Belt (Dai, 2011; Yan et al., 2011). This erosion effect has exhumed the majority  
631 of the traps and reservoirs within the the petroleum systems (Fig. 7D).

632

### 633 **7. Implications and Conclusions**

634 Combining the bitumen and present day oil seep organic geochemistry and Re-Os  
635 isotope geochronology from Kuangshanliang area we provide quantitative constraints  
636 on the petroleum evolution within the northern Longmen Shan Thrust Belt and adjacent  
637 basins that record a similar temporal tectonic evolution. The organic geochemistry of all  
638 the bitumen in the Kuangshanliang area from both dykes and fault/fractures possess  
639 similar characteristic and suggest they are sourced from shales of the Late  
640 Neoproterozoic to Early Cambrian Doushantuo and Qiongzhusi formations. In contrast,  
641 the few organic geochemistry of the present day oil seeps indicate the oil seeps possess  
642 distinct characteristics in comparison to the bitumen (e.g., lower tT24/TR26 (~0.5)  
643 value, higher GAM/H<sub>30</sub> (3.9-7.6), DH<sub>30</sub>/H<sub>30</sub> (3.1-5.5) ratio and δ<sup>13</sup>C (-25.9 ‰ to -  
644 27.7 ‰) and are suggestive of being derived from the Permian Dalong Formation.

645 The Re-Os isotope analysis showed that the Kuangshanliang area bitumen which has  
646 been derived from liquid hydrocarbon has two distinct episodes of generation. The Re-  
647 Os data for bitumen from Dyke 1 and 3 yield a date of ca. 486 Ma. This Latest  
648 Cambrian to Earliest Ordovician age agrees well with previous understanding that the  
649 Late Neoproterozoic – Early Cambrian shales of the Doushantuo and Qiongzhusi  
650 formations in the Longmen Shan Thrust Belt and adjacent Sichuan Basin first entered

651 into the oil window during the Ordovician based on basin burial modeling, and source  
652 rock maturation history (Liu et al., 2009; Yuan et al., 2012; Zhou et al., 2013). In  
653 contrast, the Re-Os data of bitumen from Dyke 2 and the fault/fractures yield a Middle  
654 Jurassic age (ca. 172 - 162 Ma). This Middle Jurassic age is coincident with the timing  
655 of the Indosinian-Yanshan orogenies (Arne et al., 1997; Jin et al., 2009b; Liu et al.,  
656 1996; Yan et al., 2003), which lead to the second phase of oil generation from the shales  
657 of the Late Neoproterozoic Doushantuo and Early Cambrian Qiongzhusi formations  
658 (Liu et al., 2009; Zou et al., 2014b). Additionally, the timing is in agreement with the  
659 basin modelling and the homogenization temperatures (~120 °C) of fluid inclusions in  
660 dolomite and quartz from the adjacent Sichuan Basin showing oil generation and  
661 migration occurred between the Triassic and Jurassic (Ma et al., 2007a; Tang et al.,  
662 2004; Zou et al., 2014b).

663 This research shows that Re-Os isotope analyses of bitumen have the potential to record  
664 multiple oil generation episodes in complex tectonic settings. In addition to the  
665 Longmen Shan Thrust Belt and the adjacent Sichuan Basin, multiple hydrocarbon  
666 generation phases related to tectonism are also reported in the Maracaibo Basin of  
667 Venezuela (Eocene and Miocene to present two continuous oil generation episodes)  
668 (Lugo and Mann, 1995; Talukdar et al., 1986) and the Tarim Basin of Northwest China  
669 (two phases of oil generation during the Late Silurian and Late Permian) (Xin et al.,  
670 2011). Thus, hydrocarbon (bitumen and oil) Re-Os chronology could aid in  
671 quantitatively constraining the petroleum evolution in basins worldwide, which may  
672 enhance our understanding of both the temporal and spatial evolution of a hydrocarbon  
673 system.

674

675 **References**

- 676 Arne, D., B. Worley, C. Wilson, S. F. Chen, D. Foster, Z. L. Luo, S. G. Liu, and P.  
677 Dirks, 1997, Differential exhumation in response to episodic thrusting along the  
678 eastern margin of the Tibetan Plateau: *Tectonophysics*, v. 280, p. 239-256.
- 679 Boles, J. R., P. Eichhubl, G. Garven, and J. Chen, 2004, Evolution of a hydrocarbon  
680 migration pathway along basin-bounding faults: Evidence from fault cement:  
681 *AAPG bulletin*, v. 88, p. 947-970.
- 682 Bordenave, M., and J. Hegre, 2005, The influence of tectonics on the entrapment of oil  
683 in the Dezful Embayment, Zagros Foldbelt, Iran: *Journal of Petroleum Geology*,  
684 v. 28, p. 339-368.
- 685 Burchfiel, B. C., C. Zhiliang, L. Yupinc, and L. H. Royden, 1995, Tectonics of the  
686 Longmen Shan and Adjacent Regions, Central China: *International Geology*  
687 *Review*, v. 37, p. 661-735.
- 688 Chen, S., C. J. Wilson, and B. A. Worley, 1995, Tectonic transition from the Songpan -  
689 Garzê Fold Belt to the Sichuan Basin, south - western China: *Basin Research*, v.  
690 7, p. 235-253.
- 691 Chen, S. F., C. Wilson, Z. L. Luo, and Q. D. Deng, 1994, The evolution of the western  
692 Sichuan foreland basin, southwestern China: *Journal of Southeast Asian Earth*  
693 *Sciences*, v. 10, p. 159-168.
- 694 Chen, S. F., and C. J. Wilson, 1996, Emplacement of the Longmen Shan Thrust—  
695 Nappe Belt along the eastern margin of the Tibetan Plateau: *Journal of Structural*  
696 *Geology*, v. 18, p. 413-430.
- 697 Chen, Z., D. Jia, G. Wei, B. Li , Q. Zeng, and Q. Hu, 2005, Structural analysis of  
698 Kuangshanliang in the northern Longmenshan fold-thrust belt and its  
699 hydrocarbon exploration: *Earth Science Frontiers*, v. 12, p. 445-450.
- 700 Cohen, A. S., A. L. Coe, J. M. Bartlett, and C. J. Hawkesworth, 1999, Precise Re–Os  
701 ages of organic-rich mudrocks and the Os isotope composition of Jurassic  
702 seawater: *Earth and Planetary Science Letters*, v. 167, p. 159-173.
- 703 Cole, G. A., R. J. Drozd, R. A. Sedivy, and H. I. Halpern, 1987, Organic geochemistry  
704 and oil-source correlations, Paleozoic of Ohio: *AAPG Bulletin*, v. 71, p. 788-  
705 809.
- 706 Cumming, V. M., D. Selby, P. G. Lillis, and M. D. Lewan, 2014, Re–Os geochronology  
707 and Os isotope fingerprinting of petroleum sourced from a Type I lacustrine  
708 kerogen: Insights from the natural Green River petroleum system in the Uinta  
709 Basin and hydrous pyrolysis experiments: *Geochimica et Cosmochimica Acta*,  
710 v. 138, p. 32-56.
- 711 Dai, H., S. Liu, W. Sun, K. Han, Z. Luo, Z. Xie, and Y. Huang, 2009, Study on  
712 characteristics of Sinian-Silurian bitumen outcrops in the Longmenshan-  
713 Micangshan area, Southwest China: *Journal of Chengdu University of*  
714 *Technology (Science & Technology Edition)*, v. 36, p. 687-696.
- 715 Dai, J., 2011, Analysis on Strcutural Deformation Stages and Dynamic Genesis of  
716 Thrust Belt in Longmen Mountain: *Journal of Southwest Petroleum University*,  
717 v. 33, p. 61-67.
- 718 De Grande, S., F. A. Neto, and M. Mello, 1993, Extended tricyclic terpanes in  
719 sediments and petroleums: *Organic geochemistry*, v. 20, p. 1039-1047.



- 720 Deng, B., S. Liu, L. Jansa, J. Cao, Y. Cheng, Z. Li, and S. Liu, 2012, Sedimentary  
721 record of Late Triassic transpressional tectonics of the Longmenshan thrust belt,  
722 SW China: *Journal of Asian Earth Sciences*, v. 48, p. 43-55.
- 723 Didyk, B., 1978, Organic geochemical indicators of palaeoenvironmental conditions of  
724 sedimentation: *Nature*, v. 272, p. 16.
- 725 Dirks, P., C. Wilson, S. Chen, Z. Luo, and S. Liu, 1994, Tectonic evolution of the NE  
726 margin of the Tibetan Plateau; evidence from the central Longmen Mountains,  
727 Sichuan Province, China: *Journal of Southeast Asian Earth Sciences*, v. 9, p.  
728 181-192.
- 729 Esser, B. K., and K. K. Turekian, 1993, The Osmium Isotopic Composition of the  
730 Continental-Crust: *Geochimica Et Cosmochimica Acta*, v. 57, p. 3093-3104.
- 731 Fall, A., P. Eichhubl, R. J. Bodnar, S. E. Laubach, and J. S. Davis, 2015, Natural  
732 hydraulic fracturing of tight-gas sandstone reservoirs, Piceance Basin, Colorado:  
733 *Geological Society of America Bulletin*, v. 127, p. 61-75.
- 734 Feng, C., Q. Chen, C. Tan, X. Qin, P. Zhang, and W. Meng, 2014, The stress state of the  
735 Beichuan-Jiangyou segment of the Longmenshan fault before and after the  
736 Wenchuan M S 8.0 Earthquake: *Journal of Earth Science*, v. 25, p. 861-870.
- 737 Finlay, A. J., D. Selby, and M. J. Osborne, 2011, Re-Os geochronology and  
738 fingerprinting of United Kingdom Atlantic margin oil: Temporal implications  
739 for regional petroleum systems: *Geology*, v. 39, p. 475-478.
- 740 Finlay, A. J., D. Selby, and M. J. Osborne, 2012, Petroleum source rock identification of  
741 United Kingdom Atlantic Margin oil fields and the Western Canadian Oil Sands  
742 using Platinum, Palladium, Osmium and Rhenium: Implications for global  
743 petroleum systems: *Earth and Planetary Science Letters*, v. 313, p. 95-104.
- 744 Ge, X., C. Shen, D. Selby, D. Deng, and L. Mei, 2016, Apatite fission-track and Re-Os  
745 geochronology of the Xuefeng uplift, China: Temporal implications for dry gas  
746 associated hydrocarbon systems: *Geology*, v. 44, p. 491-494.
- 747 Georgiev, S. V., H. J. Stein, J. L. Hannah, R. Galimberti, M. Nali, G. Yang, and A.  
748 Zimmerman, 2016, Re-Os dating of maltenes and asphaltenes within single  
749 samples of crude oil: *Geochimica et Cosmochimica Acta*, v. 179, p. 53-75.
- 750 Gramlich, J. W., T. J. Murphy, E. L. Garner, and W. R. Shields, 1973, Absolute Isotopic  
751 Abundance Ratio and Atomic Weight of a Reference Sample of Rhenium:  
752 *Journal of research of the Notional Bureau of Standards - A. Physics and*  
753 *Chemistry*, v. 77A, p. 691-698.
- 754 Hackley, P. C., R. T. Ryder, M. H. Trippi, and H. Alimi, 2013, Thermal maturity of  
755 northern Appalachian Basin Devonian shales: insights from sterane and terpane  
756 biomarkers: *Fuel*, v. 106, p. 455-462.
- 757 Harrowfield, M. J., and C. J. Wilson, 2005, Indosinian deformation of the Songpan  
758 Garze fold belt, northeast Tibetan Plateau: *Journal of Structural Geology*, v. 27,  
759 p. 101-117.
- 760 Huang, D., and L. Wang, 2008, Geochemical characteristics of bituminous dike in  
761 Kuangshanliang area of the Northwestern Sichuan Basin and its significance:  
762 *Acta Petrolei Sinica*, v. 29, p. 23-28.
- 763 Huang, M., R. Maas, I. Buick, and I. Williams, 2003, Crustal response to continental  
764 collisions between the Tibet, Indian, South China and North China blocks:  
765 Geochronological constraints from the Songpan - Garze orogenic belt, western  
766 China: *Journal of Metamorphic Geology*, v. 21, p. 223-240.

- 767 Huang, W., S. Liu, G. Xu, G. Wang, W. Ma, C. Zhang, and G. Song, 2011,  
768 Characteristics of paleo oil pools from Sinian to Lower Paleozoic in  
769 southeastern margin of Sichuan Basin: *Geological Review*, v. 57, p. 285-299.
- 770 Hwang, R., S. Teerman, and R. Carlson, 1998, Geochemical comparison of reservoir  
771 solid bitumens with diverse origins: *Organic Geochemistry*, v. 29, p. 505-517.
- 772 Jia, D., G. Wei, Z. Chen, B. Li, Q. Zeng, and G. Yang, 2006, Longmen Shan fold-thrust  
773 belt and its relation to the western Sichuan Basin in central China: New insights  
774 from hydrocarbon exploration: *AAPG Bulletin*, v. 90, p. 1425-1447.
- 775 Jiang, S.-Y., J.-H. Yang, H.-F. Ling, Y.-Q. Chen, H.-Z. Feng, K.-D. Zhao, and P. Ni,  
776 2007, Extreme enrichment of polymetallic Ni-Mo-PGE-Au in Lower Cambrian  
777 black shales of South China: An Os isotope and PGE geochemical investigation:  
778 *Palaeogeography, Palaeoclimatology, Palaeoecology*, v. 254, p. 217-228.
- 779 Jin, W., L. Tang, K. Yang, G. Wan, and Z. Lü, 2010, Segmentation of the Longmen  
780 Mountains thrust belt, western Sichuan foreland basin, SW China:  
781 *Tectonophysics*, v. 485, p. 107-121.
- 782 Jin, W., L. Tang, K. Yang, G. Wan, Z. Lü, and Y. Yu, 2009a, Transfer zones within the  
783 Longmen Mountains thrust belt, SW China: *Geosciences Journal*, v. 13, p. 1-14.
- 784 Jin, W., L. Tang, K. Yang, G. Wan, and Z. Lu, 2008, Progress and problem of study on  
785 characters of the Longmen Mountain thrust belt: *Geological Review*, v. 54, p.  
786 37-46.
- 787 Jin, W., L. Tang, K. Yang, G. Wan, Z. Lv, and Y. Yu, 2009b, Tectonic evolution of the  
788 middle frontal area of the Longmen Mountain thrust belt, western Sichuan basin,  
789 China: *Acta Geologica Sinica (English Edition)*, v. 83, p. 92-102.
- 790 Kendall, B., R. A. Creaser, and D. Selby, 2009, 187Re-187Os geochronology of  
791 Precambrian organic-rich sedimentary rocks: *Geological Society, London,*  
792 *Special Publications*, v. 326, p. 85-107.
- 793 Lei, Y., C. Jia, B. Li, G. Wei, Z. Chen, and X. Shi, 2012, Meso - Cenozoic Tectonic  
794 Events Recorded by Apatite Fission Track in the Northern Longmen - Micang  
795 Mountains Region: *Acta Geologica Sinica (English edition)*, v. 86, p. 153-165.
- 796 Li, C., L. Wen, and S. Tao, 2015, Characteristics and enrichment factors of supergiant  
797 Lower Cambrian Longwangmiao gas reservoir in Anyue gas field: the oldest and  
798 largest single monoblock gas reservoir in China: *Energy, Exploration &*  
799 *Exploitation*, v. 33, p. 827-850.
- 800 Li, J., Z. Li, and P. Wang, 2012, The preliminary analysis of structure pattern of  
801 Longmeshan tectonic zone of Sichuan: *Yunnan Geology*, v. 31, p. 272-276.
- 802 Li, J., Z. Wang, and M. Zhao, 1999, 40Ar/39Ar Thermochronological Constraints on  
803 the Timing of Collisional Orogeny in the Mian - Lue Collision Belt, Southern  
804 Qinling Mountains: *Acta Geologica Sinica (English edition)*, v. 73, p. 208-215.
- 805 Li, X., Z. Wang, X. Zhang, Q. Liu, and J. Yan, 2001, Charactersitics of Paleo-Uplifts in  
806 Sichuan Basin and their control on natural gases: *Oil & Gas Geology*, v. 22, p.  
807 347-351.
- 808 Li, Z., S. Liu, H. Chen, S. Liu, B. Guo, and X. Tian, 2008, Structural segmentation and  
809 zonation and differential deformation across and along the Longmen thrust belt,  
810 West Sichuan: *Journal of Chengdu University of Technology (Science &*  
811 *Technology Edition)*, v. 35, p. 440-455.
- 812 Liang, D., 2007, Evaluation on Efficient Source Rock of Complex Structure Area in  
813 Southern China, The China Petroleum & Chemical Corporation.

- 814 Lillis, P. G., and D. Selby, 2013, Evaluation of the rhenium–osmium geochronometer in  
815 the Phosphoria petroleum system, Bighorn Basin of Wyoming and Montana,  
816 USA: *Geochimica et Cosmochimica Acta*, v. 118, p. 312-330.
- 817 Lin, J., Y. Xie, J. Liu, Z. Zhao, X. Jing, and H. Cheng, 2011, Restudy of the source rock  
818 of Majiang paleo-reservoir: *Geological Science and Technology Information*, v.  
819 30, p. 105-109.
- 820 Liu, G., S. Wang, W. Pan, and J. Lv, 2003, Characteristics of Tianjingshan destroyed oil  
821 reservoir in Guangyuan Area, Sichuan: *Marine Origin Petroleum Geology*, v. 8,  
822 p. 103-108.
- 823 Liu, Q., D. Zhu, Z. Jin, C. Liu, D. Zhang, and Z. He, 2016, Coupled alteration of  
824 hydrothermal fluids and thermal sulfate reduction (TSR) in ancient dolomite  
825 reservoirs—An example from Sinian Dengying Formation in Sichuan Basin,  
826 southern China: *Precambrian Research*, v. 285, p. 39-57.
- 827 Liu, S., B. Deng, Z. Li, and W. Sun, 2011, The texture of sedimentary basin-orogeny  
828 belt system and its influence on oil/gas distribution: A case study from Sichuan  
829 basin: *Acta Petrologica Sinica*, v. 27, p. 621-635.
- 830 Liu, S., Z. Luo, S. Dai, D. Arne, and C. Wilson, 1996, The uplift of the Longmenshan  
831 thrust belt and subsidence of the west Sichuan Foreland Basin: *Acta Geologica  
832 Sinica (English Edition)*, v. 9, p. 16-26.
- 833 Liu, S., Y. Ma, X. Cai, G. Xu, G. Wang, Z. Yong, W. Sun, H. Yuan, and C. Pan, 2009,  
834 Characteristic and accumulation process of the natural gas from Sinian to Lower  
835 Paleozoic in Sichuan Basin: China. *Journal of Chengdu University of  
836 Technology (Science & Technology Edition)*, v. 33, p. 345-354.
- 837 Liu, S., R. Steel, and G. Zhang, 2005, Mesozoic sedimentary basin development and  
838 tectonic implication, northern Yangtze Block, eastern China: record of  
839 continent–continent collision: *Journal of Asian Earth Sciences*, v. 25, p. 9-27.
- 840 Liu, S., X. Zhao, Z. Luo, G. Xu, and G. Wang, 2001, Study on the tectonic events in the  
841 system of the Longmen Mountain-west Sichuan foreland basin, China: *Journal  
842 of Chengdu University of Technology*, v. 28, p. 221-230.
- 843 Ludwig, K., 2003, A plotting and regression program for radiogenic-isotope data,  
844 version 3.00: United State Geol Survey, open file report, p. 1-70.
- 845 Lugo, J., and P. Mann, 1995, Jurassic-Eocene tectonic evolution of Maracaibo basin,  
846 Venezuela: *AAPG Special Volumes*, p. 699-725.
- 847 Ma, Y., X. Cai, and T. Guo, 2007a, The controlling factors of oil and gas charging and  
848 accumulation of Puguang gas field in the Sichuan Basin: *Chinese Science  
849 Bulletin*, v. 52, p. 193-200.
- 850 Ma, Y., X. Cai, P. Zhao, Y. Luo, and X. Zhang, 2010, Distribution and further  
851 exploration of the Large-medium sized gas field in Sichuan Basin: *Acta  
852 Geologica Sinica*, v. 31, p. 347-354.
- 853 Ma, Y., X. Guo, T. Guo, R. Huang, X. Cai, and G. Li, 2007b, The Puguang gas field:  
854 New giant discovery in the mature Sichuan Basin, southwest China: *AAPG  
855 bulletin*, v. 91, p. 627-643.
- 856 Moretti, I., P. Baby, E. Mendez, and D. Zubieta, 1996, Hydrocarbon generation in  
857 relation to thrusting in the Sub Andean zone from 18 to 22 degrees S, Bolivia:  
858 *Petroleum Geoscience*, v. 2, p. 17-28.
- 859 Nowell, G., D. Pearson, S. Parman, A. Luguét, and E. Hanski, 2008, Precise and  
860 accurate  $^{186}\text{Os}/^{188}\text{Os}$  and  $^{187}\text{Os}/^{188}\text{Os}$  measurements by multi-collector  
861 plasma ionisation mass spectrometry, part II: Laser ablation and its application

862 to single-grain Pt–Os and Re–Os geochronology: *Chemical Geology*, v. 248, p.  
863 394-426.

864 Parnell, J., and I. Swainbank, 1990, Pb-Pb dating of hydrocarbon migration into a  
865 bitumen-bearing ore deposit, North Wales: *Geology*, v. 18, p. 1028-1030.

866 Peters, K., C. Walters, and J. Moldowan, 2005, *The Biomarker guide, biomarkers and*  
867 *isotopes in petroleum exploration and earth history*, vol 1–2, Cambridge  
868 University Press, New York, 961 p.

869 Peters, K. E., and J. M. Moldowan, 1993, *The biomarker guide: interpreting molecular*  
870 *fossils in petroleum and ancient sediments: United States*, Englewood Cliffs, NJ  
871 (United States); Prentice Hall.

872 Pusey, W. C., 1973, How to evaluate potential gas and oil source rocks: *World Oil*, v.  
873 176, p. 71-75.

874 Rao, D., J. Qin, Tenger, and M. Zhang, 2008, Source analysis of oil seepage and  
875 bitumen originating from marine layer strata in Guangyuan area, the northwest  
876 Sichuan Basin: *Petroleum Geology & Experiment*, v. 30, p. 596-599.

877 Ravizza, G., and K. Turekian, 1992, The osmium isotopic composition of organic-rich  
878 marine sediments: *Earth and Planetary Science Letters*, v. 110, p. 1-6.

879 Rooney, A., 2011, Re-Os geochronology and geochemistry of Proterozoic sedimentary  
880 successions, Durham University, Durham, 114 p.

881 Rooney, A. D., D. Selby, J.-P. Houzay, and P. R. Renne, 2010, Re–Os geochronology  
882 of a Mesoproterozoic sedimentary succession, Taoudeni basin, Mauritania:  
883 implications for basin-wide correlations and Re–Os organic-rich sediments  
884 systematics: *Earth and Planetary Science Letters*, v. 289, p. 486-496.

885 Seifert, W., and J. Moldowan, 1986, Use of biological markers in petroleum  
886 exploration: *Methods in geochemistry and geophysics*, v. 24, p. 261-290.

887 Selby, D., and R. A. Creaser, 2005, Direct radiometric dating of hydrocarbon deposits  
888 using rhenium-osmium isotopes: *Science*, v. 308, p. 1293-1295.

889 Selby, D., R. A. Creaser, K. Dewing, and M. Fowler, 2005, Evaluation of bitumen as a  
890 <sup>187</sup>Re–<sup>187</sup>Os geochronometer for hydrocarbon maturation and migration: A  
891 test case from the Polaris MVT deposit, Canada: *Earth and Planetary Science*  
892 *Letters*, v. 235, p. 1-15.

893 Selby, D., R. A. Creaser, and M. G. Fowler, 2007, Re–Os elemental and isotopic  
894 systematics in crude oils: *Geochimica et Cosmochimica Acta*, v. 71, p. 378-386.

895 Smoliar, M. I., R. J. Walker, and J. W. Morgan, 1996, Re-Os ages of group IIA, IIIA,  
896 IVA, and IVB iron meteorites: *Science*, v. 271, p. 1099-1102.

897 Summons, R. E., J. M. Hope, R. Swart, and M. R. Walter, 2008, Origin of Nama Basin  
898 bitumen seeps: Petroleum derived from a Permian lacustrine source rock  
899 traversing southwestern Gondwana: *Organic Geochemistry*, v. 39, p. 589-607.

900 Sun, D., 2011, The structural character and Meso-Cenozoic evolution of Micang  
901 Mountain structural zone, Northern Sichuan basin, China, Chengdu University  
902 of Technology, Chengdu, 206 p.

903 Sun, W., S. Liu, K. Han, Z. Luo, G. Wang, and G. Xu, 2009, The Petroleum Geological  
904 Condition and Exploration Prospect Analysis in Sinian, Sichuan Basin:  
905 *Petroleum Geology & Experiment*, v. 31, p. 350-355.

906 Talukdar, S., O. Gallango, and M. Chin-A-Lien, 1986, Generation and migration of  
907 hydrocarbons in the Maracaibo Basin, Venezuela: An integrated basin study:  
908 *Organic Geochemistry*, v. 10, p. 261-279.

- 909 Tang, J., T. Zhang, Z. Bao, and M. Zhang, 2004, Study of Organic Inclusion in the  
910 Carbonate Reservoir Bed of the Weiyuan Gas Field in the Sichuan Basin:  
911 Geological Review, v. 50, p. 210-214.
- 912 Tian, X., 2009, Structural Features in the northern segment of Longmen Mountains and  
913 the discussion on its hydrocarbon prospects, Chengdu University of Technology,  
914 Chengdu, 91 p.
- 915 Tissot, B. P., and D. H. Welte, 1984, Petroleum formation and occurrence: Other  
916 Information: From review by Edward A. Beaumont, in The American  
917 Association of Petroleum Geologists Bulletin, Vol. 71, No. 4 (April 1987),  
918 Medium: X; Size: Pages: 699 p.
- 919 Urien, C. M., J. Zambrano, and M. Yrigoyen, 1995, Petroleum basins of southern South  
920 America: an overview: AAPG Bulletin, v. special, p. 63-77.
- 921 Wang, L., K. Han, B. Xie, J. Zhang, M. Du, M. Wan, and D. Li, 2005, Reservoiring  
922 conditions of the oil and gas fields in the North section of Longmen Mountain  
923 Nappe structural belts: Natural Gas Industry, v. 25, p. 1-5.
- 924 Wang, M., C. Bao, and M. Xiao, 1989, Petroleum Geology of China (Vol. 10) Sichuan  
925 Oil & Gas Field v. 10, Petroleum Industry Press (Beijing), 516 p.
- 926 Wang, S., and X. Li, 1999, Geochemistry of the Sinian natural gases and petroleum  
927 systems in the Weiyuan–Ziyuan area: Natural Gas Geosciences Journal, v. 10, p.  
928 63-69.
- 929 Wang, S., B. Zheng, and L. Cai, 1997, The Destroyed Oil Pools in South China and  
930 Hydrocarbon Prospecting: Marine Origin Petroleum Geology, v. 2, p. 44-50.
- 931 Wang, Y., W. Fan, G. Zhao, S. Ji, and T. Peng, 2007, Zircon U–Pb geochronology of  
932 gneissic rocks in the Yunkai massif and its implications on the Caledonian event  
933 in the South China Block: Gondwana Research, v. 12, p. 404-416.
- 934 Wang, Y., S. Liu, B. Fu, and S. Xing, 2015, Quantitative estimation of surface  
935 denudation in Longmen Shan during late cenozoic: Earth Science - Journal of  
936 China University of Geosciences, v. 40, p. 953-964.
- 937 Wei, G., G. Chen, S. Du, L. Zhang, and W. Yang, 2008, Petroleum systems of the oldest  
938 gas field in China: Neoproterozoic gas pools in the Weiyuan gas field, Sichuan  
939 Basin: Marine and Petroleum Geology, v. 25, p. 371-386.
- 940 Wenger, L. M., and G. H. Isaksen, 2002, Control of hydrocarbon seepage intensity on  
941 level of biodegradation in sea bottom sediments: Organic Geochemistry, v. 33,  
942 p. 1277-1292.
- 943 Wilson, C. J., M. J. Harrowfield, and A. J. Reid, 2006, Brittle modification of Triassic  
944 architecture in eastern Tibet: implications for the construction of the Cenozoic  
945 plateau: Journal of Asian Earth Sciences, v. 27, p. 341-357.
- 946 Worley, B. A., and C. J. Wilson, 1996, Deformation partitioning and foliation  
947 reactivation during transpressional orogenesis, an example from the Central  
948 Longmen Shan, China: Journal of Structural Geology, v. 18, p. 395-411.
- 949 Wu, L., Y. Liao, Y. Fang, and A. Geng, 2012, The study on the source of the oil seeps  
950 and bitumens in the Tianjingshan structure of the northern Longmen Mountain  
951 structure of Sichuan Basin, China: Marine and Petroleum Geology, v. 37, p.  
952 147-161.
- 953 Xie, B., L. Wang, J. Zhang, and S. Chen, 2003, Vertical Distribution and Geochemical  
954 Behaviours of the Hydrocarbon Source Rocks in the North Section of Longmen  
955 Mountains: Natural Gas Industry, v. 23, p. 21-24.

- 956 Xin, Y., N. Qiu, J. Qin, and L. Zheng, 2011, Study on Second Hydrocarbon Generation  
957 of Ordovician Hydrocarbon Source Rock in Tarim Basin: *Journal of Earth*  
958 *Science and Environment*, v. 33, p. 261-267.
- 959 Xu, G., J. L. Hannah, H. J. Stein, B. Bingen, G. Yang, A. Zimmerman, W. Weitschat,  
960 A. Mørk, and H. M. Weiss, 2009, Re–Os geochronology of Arctic black shales  
961 to evaluate the Anisian–Ladinian boundary and global faunal correlations: *Earth*  
962 *and Planetary Science Letters*, v. 288, p. 581-587.
- 963 Xu, G., J. L. Hannah, H. J. Stein, A. Mørk, J. O. Vigran, B. Bingen, D. L. Schutt, and B.  
964 A. Lundschieen, 2014, Cause of Upper Triassic climate crisis revealed by Re–Os  
965 geochemistry of Boreal black shales: *Palaeogeography, Palaeoclimatology,*  
966 *Palaeoecology*, v. 395, p. 222-232.
- 967 Yahi, N., R. G. Schaefer, and R. Littke, 2001, Petroleum generation and accumulation  
968 in the Berkine basin, eastern Algeria: *AAPG bulletin*, v. 85, p. 1439-1467.
- 969 Yan, D., M. Zhou, S. Li, and G. Wei, 2011, Structural and geochronological constraints  
970 on the Mesozoic-Cenozoic tectonic evolution of the Longmen Shan thrust belt,  
971 eastern Tibetan Plateau: *Tectonics*, v. 30, p. 1-24.
- 972 Yan, D., M. Zhou, H. Song, X. Wang, and J. Malpas, 2003, Origin and tectonic  
973 significance of a Mesozoic multi-layer over-thrust system within the Yangtze  
974 Block (South China): *Tectonophysics*, v. 361, p. 239-254.
- 975 Yang, C., Z. Wang, B. P. Hollebone, C. E. Brown, and M. Landriault, 2009,  
976 Characteristics of bicyclic sesquiterpanes in crude oils and petroleum products:  
977 *Journal of Chromatography A*, v. 1216, p. 4475-4484.
- 978 Yuan, H., J. Liang, D. Gong, G. Xu, S. Liu, and G. Wang, 2012, Formation and  
979 evolution of Sinian oil and gas pools in typical structures, Sichuan Basin, China:  
980 *Petroleum Science*, v. 9, p. 129-140.
- 981 Zhang, L., G. Wei, S. Wu, Z. Wang, X. Xiao, P. Zhang, and Y. Shen, 2005, Distribution  
982 Characters and Hydrocarbon-Generating Potential of Bitumen of Sinian-Lower  
983 Palaeozoic in Sichuan Basin: *Petroleum Geology and Experiment* v. 27, p. 276-  
984 280.
- 985 Zhang, S., A. Hanson, J. Moldowan, S. Graham, D. Liang, E. Chang, and F. Fago, 2000,  
986 Paleozoic oil–source rock correlations in the Tarim basin, NW China: *Organic*  
987 *Geochemistry*, v. 31, p. 273-286.
- 988 Zhang, S., and G. Zhu, 2006, Gas accumulation characteristics and exploration potential  
989 of marine sediments in Sichuan Basin: *Acta Petrolei Sinica*, v. 27, p. 1-8.
- 990 Zhou, Q., X. Xiao, H. Tian, and R. Wilkins, 2013, Oil charge history of bitumens of  
991 differing maturities in exhumed Palaeozoic reservoir rocks at Tianjingshan, NW  
992 Sichuan Basin, southern China: *Journal of Petroleum Geology*, v. 36, p. 363-  
993 382.
- 994 Zhu, B., J. Zhang, X. Tu, X. Chang, C. Fan, Y. Liu, and J. Liu, 2001, Pb, Sr, and Nd  
995 isotopic features in organic matter from China and their implications for  
996 petroleum generation and migration: *Geochimica et Cosmochimica Acta*, v. 65,  
997 p. 2555-2570.
- 998 Zhuang, G., 1985, Regional geology of Guangxi Zhuang Autonomous Region,  
999 Geological Publishing House, 853 p.
- 1000 Zou, C., J. Du, C. Xu, Z. Wang, B. Zhang, G. Wei, T. Wang, G. Yao, S. Deng, and J.  
1001 Liu, 2014a, Formation, distribution, resource potential, and discovery of Sinian–  
1002 Cambrian giant gas field, Sichuan Basin, SW China: *Petroleum Exploration and*  
1003 *Development*, v. 41, p. 306-325.

1004 Zou, C., G. Wei, C. Xu, J. Du, Z. Xie, Z. Wang, L. Hou, C. Yang, J. Li, and W. Yang,  
1005 2014b, Geochemistry of the Sinian–Cambrian gas system in the Sichuan Basin,  
1006 China: Organic Geochemistry, v. 74, p. 13-21.  
1007 Zumberge, J. E., 1987, Prediction of source rock characteristics based on terpane  
1008 biomarkers in crude oils: A multivariate statistical approach: Geochimica et  
1009 Cosmochimica Acta, v. 51, p. 1625-1637.  
1010

1011 **Author's vita**

1012 **Xiang Ge**

1013 Key Laboratory of Tectonics and Petroleum Resources (China University of  
1014 Geosciences), Ministry of Education, Wuhan, 430074, China; 388 Lumo Road,  
1015 Hongshan District, Wuhan City, Hubei Province, China.

1016 Department of Earth Sciences, Durham University, Durham, DH1 3LE, UK; Arthur  
1017 Holmes Building, Science Site, South Road, Durham, England, UK

1018 [xiangge89@126.com](mailto:xiangge89@126.com)

1019 Xiang Ge is a Joint Ph.D student at the China University of Geoscience (Wuhan) and  
1020 Durham University. He received his B.Sc. and M.Sc. from China University of  
1021 Geoscience (Wuhan). His PhD thesis is focusing on the petroleum geology of the  
1022 Sichuan Basin applying hydrocarbon Re-Os isotope, structural and tectonic analyses.

1023

1024 **Chuanbo Shen (\*Corresponding author)**

1025 Key Laboratory of Tectonics and Petroleum Resources (China University of  
1026 Geosciences), Ministry of Education, Wuhan, 430074, China; 388 Lumo Road,  
1027 Hongshan District, Wuhan City, Hubei Province, China.

1028 [cugshen@126.com](mailto:cugshen@126.com)

1029 Chuanbo Shen is currently a professor in the Faculty of Earth Resources at the China  
1030 University of Geosciences (Wuhan). He received his B.Sc., M.Sc., and Ph.D. from

1031 China University of Geoscience (Wuhan). He also completed postdoctoral research in  
1032 Technische Universität Bergakademie Freiberg, Germany. His present research interests  
1033 are low-temperature thermochronology, tectonic-thermal evolution and hydrocarbon  
1034 geochronology.

1035

1036 **David Selby**

1037 Department of Earth Sciences, Durham University, Durham, DH1 3LE, UK

1038 [david.selby@durham.ac.uk](mailto:david.selby@durham.ac.uk)

1039 David Selby is a Professor of Earth Sciences at Durham University, UK. He received a  
1040 bachelor's degree in geology from Southampton University, UK and Ph.D. degree from  
1041 the University of Alberta, Canada. He also carried out his postdoctoral research at the  
1042 University of Alberta. His research focuses on the Earth Science disciplines of  
1043 economic geology, petroleum geoscience and paleoclimate / oceanography, principally  
1044 through the application and development of the novel, state-of-the-art, rhenium-osmium  
1045 radio isotope methodology.

1046

1047 **Jie Wang**

1048 Wuxi institute of petroleum geology, SINOPEC, Wuxi, 214151, China

1049 [wangjie.syky@sinopec.com](mailto:wangjie.syky@sinopec.com)

1050 Jie Wang is now a Senior Engineer in Wuxi institute of petroleum geology, SINOPEC.  
1051 He obtained his B.Sc. degree in Petroleum Engineering from Xi'an Shiyou University  
1052 and M.Sc. and Ph.D. degree from Lanzhou Geological Institute, Chinese Academy of  
1053 Sciences. He also carried out his postdoctoral research at the Zhejiang University and  
1054 Wuxi institute of petroleum geology in 2005-2008. His current research focuses on



1055 petroleum geology and organic geochemistry.

1056

1057 **Liangbang Ma**

1058 Wuxi institute of petroleum geology, SINOPEC, Wuxi, 214151, China

1059 [malb.syky@sinopec.com](mailto:malb.syky@sinopec.com)

1060 Liangbang Ma is a Senior Engineer in Wuxi institute of petroleum geology, SINOPEC.

1061 He received his B.Sc. and M.Sc. in Analytical Chemistry from Chengdu University of

1062 Technology. His current research focuses on organic geochemistry.

1063

1064 **Xiaoyan Ruan**

1065 Key Laboratory of Tectonics and Petroleum Resources (China University of

1066 Geosciences), Ministry of Education, Wuhan, 430074, China; 388 Lumo Road,

1067 Hongshan District, Wuhan City, Hubei Province, China.

1068 [ruan6231@163.com](mailto:ruan6231@163.com)

1069 Xiaoyan Ruan is an Associate Professor in the Faculty of Earth Resources at the China

1070 University of Geosciences (Wuhan). She received her B.Sc., M.Sc., and Ph.D. from

1071 China University of Geosciences (Wuhan). She carried out research at Bryant

1072 University, in the United States as a visiting scholar in 2010-2011. Her current research

1073 focuses on biological geochemistry and petroleum geochemistry.

1074

1075 **Shouzhi Hu**

1076 Key Laboratory of Tectonics and Petroleum Resources (China University of

1077 Geosciences), Ministry of Education, Wuhan, 430074, China; 388 Lumo Road,

1078 Hongshan District, Wuhan City, Hubei Province, China.

1079 [hushzh@cug.edu.cn](mailto:hushzh@cug.edu.cn)

1080 Shouzhi Hu is an Associate Professor in the Faculty of Earth Resources at the China  
1081 University of Geosciences (Wuhan). She received her B.Sc., M.Sc., and Ph.D. in  
1082 Petroleum Geology from Southwest Petroleum University. She also completed a year  
1083 research in GFZ Department, Germany as a visiting scholar in 2012-2013. Her current  
1084 research focuses on the petroleum geology and organic geochemistry.

1085

1086 **Lianfu Mei**

1087 Key Laboratory of Tectonics and Petroleum Resources (China University of  
1088 Geosciences), Ministry of Education, Wuhan, 430074, China; 388 Lumo Road,  
1089 Hongshan District, Wuhan City, Hubei Province, China.

1090 [lfmei@cug.edu.cn](mailto:lfmei@cug.edu.cn)

1091 Lianfu Mei is a Professor in the Faculty of Earth Resources at the China University of  
1092 Geosciences (Wuhan). He received a bachelor's degree in Mineral Prospecting and  
1093 Exploration from Zhongnan University, China UK and M.Sc., and Ph.D. degree in  
1094 petroleum geology from the China University of Geosciences (Wuhan). His research  
1095 focuses on the structural geology and petroleum geoscience within petroliferous basins.

1096

1097

1098 **Figure Captions**

1099 Fig. 1. A) Regional map of the Longmen Shan Thrust Belt and the adjacent Sichuan  
1100 Basin and Songpan-Garze Belt in the SE and NW, respectively. The shaded area is  
1101 expanded in Figure 1B and 1C; B) Simplified map of the Sichuan Basin showing the  
1102 distribution of gas fields with different orogenic belts. Substantially modified after **Li et**

1103 al., 2015; Li et al., 2001; Ma et al., 2010; C) Structural map of the Longmen Shan  
1104 Thrust Belt showing the bitumen outcrop distribution, and the location of the Cambrian  
1105 cored Kuangshanliang anticline (our study area). Substantially modified after Tian,  
1106 2009.

1107

1108 Fig. 2. Stratigraphy, hydrocarbon system and tectonic events in the North Longmen  
1109 Shan area. Substantially modified after Chen and Wilson, 1996; Wu et al., 2012.

1110

1111 Fig. 3. A) Simplified geological map of the Kuangshanliang anticline; B) Detailed  
1112 geology feature in the Kuangshanliang area and locations of the bitumen and present  
1113 day oil seep samples.

1114

1115 Fig. 4. Bitumen and oil sample locations and field relationships. A) Bitumen Dyke 1  
1116 showing the relationship between the dyke and the country rock. A') detailed image of  
1117 the breccia zone shown in A. B) Bitumen sample (11SKD-3d, 11SKD-4d, 11SKD-5d,  
1118 SKD-1f) locations in Dyke 1 and related fault/fractures. C) Bitumen sample (XKD-1d,  
1119 XKD-2d) locations in Dyke 2. D) Syn / post thrust fault in Dyke 2. E) Bitumen sample  
1120 (HSCD-1d and GY1d-6d) locations in Dyke 3. F) Bitumen samples (LXB-1f, LXB-2f)  
1121 from a fault zone. G) Bitumen sample (11LXB-1f) from a fault plane. H) Present day oil  
1122 seep samples (Oil-3, Oil-5, Oil-7) occurring in the Early Cambrian Qiongzhusi  
1123 Formation.

1124

1125 Fig. 5. Total Ion Chromatogram (TIC), m/z 191 and m/z 217 mass chromatograms of  
1126 the bitumen (11SKD-4d, XKD-1d, GY-3d, HSCD-1d, LXB-1f) and the present day oil  
1127 seeps (Oil-5) in the Kuangshangliang area.

1128

1129 Fig. 6. A) Traditional  $^{187}\text{Re}/^{188}\text{Os}$  vs  $^{187}\text{Os}/^{188}\text{Os}$  plot showing all the Re-Os data for  
1130 bitumen from the dykes and faults/fractures, as well as the present day oil seeps in the  
1131 Kuangshanliang anticline (Bold for Dyke 1 bitumen; Underline for Dyke 2 bitumen;  
1132 Italic for Dyke 3 bitumen; Regular font for fault/fracture bitumen and Bold Italic for the  
1133 present day oil seeps). B) The Re-Os isotope data of Dyke 3 bitumen. C) The Re-Os  
1134 isotope data of bitumen from Dyke 1 and 3 and fault bitumen sample, 11LXB-1f. D)  
1135 The Re-Os isotope data of Dyke 1 and 3 bitumen (without HSCD-1 and GY-1). E. The  
1136 Re-Os isotope data of all Dyke 2 and fault/fracture bitumen. F) The Re-Os isotope data  
1137 of Dyke 2 and fault/fracture bitumen based on  $\text{Os}_i$  values groups ( $\sim 1.82$  and  $\sim 1.89$ ).  
1138 Data-point ellipses are shown with 2-sigma absolute uncertainty. Data labels are sample  
1139 numbers listed in Table 2.

1140

1141 Fig. 7. The relationship between petroleum generation and tectonism. Shown is a  
1142 comparison of the Re-Os ages with source rocks (Xie et al., 2003; Zhou et al., 2013),  
1143 published basin model and fluid inclusion results (Ma et al., 2007a; Tang et al., 2004)  
1144 and muscovite  $^{40}\text{Ar}/^{39}\text{Ar}$  ages (Li et al., 1999; Yan et al., 2011), Jurassic zircon fission  
1145 track ages (Arne et al., 1997) in Longmen Shan Thrust Belt. The schematic cartoon  
1146 model shows the hydrocarbon evolution in the Kuangshanliang anticline, Northern  
1147 Longmen Shan Thrust Belt. A) First phase of oil generation during the Ordovician,  
1148 before the Caledonian Orogeny. B) Oil generation ceased due to uplift caused by the

- 1149 Caledonian Orogeny (ca. 450 - 400 Ma). C) Second phase of oil generation during the
- 1150 Middle Jurassic Indosinian-Yanshan orogenies. D) Present condition of the bitumen and
- 1151 present day oil seeps after Cenozoic Himalayan Orogeny.

Figure 1

[Click here to download Figure Fig.1.eps](#)

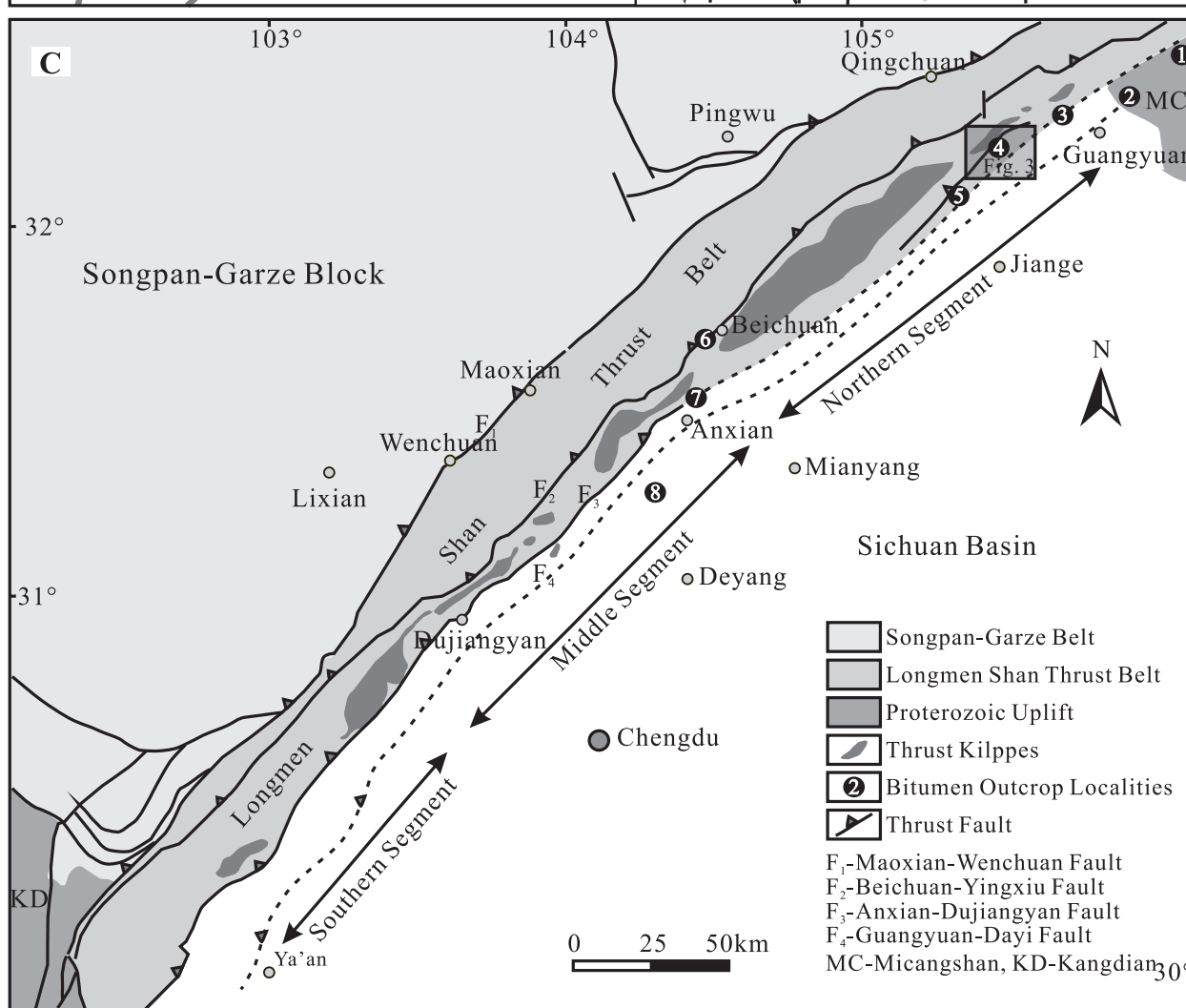
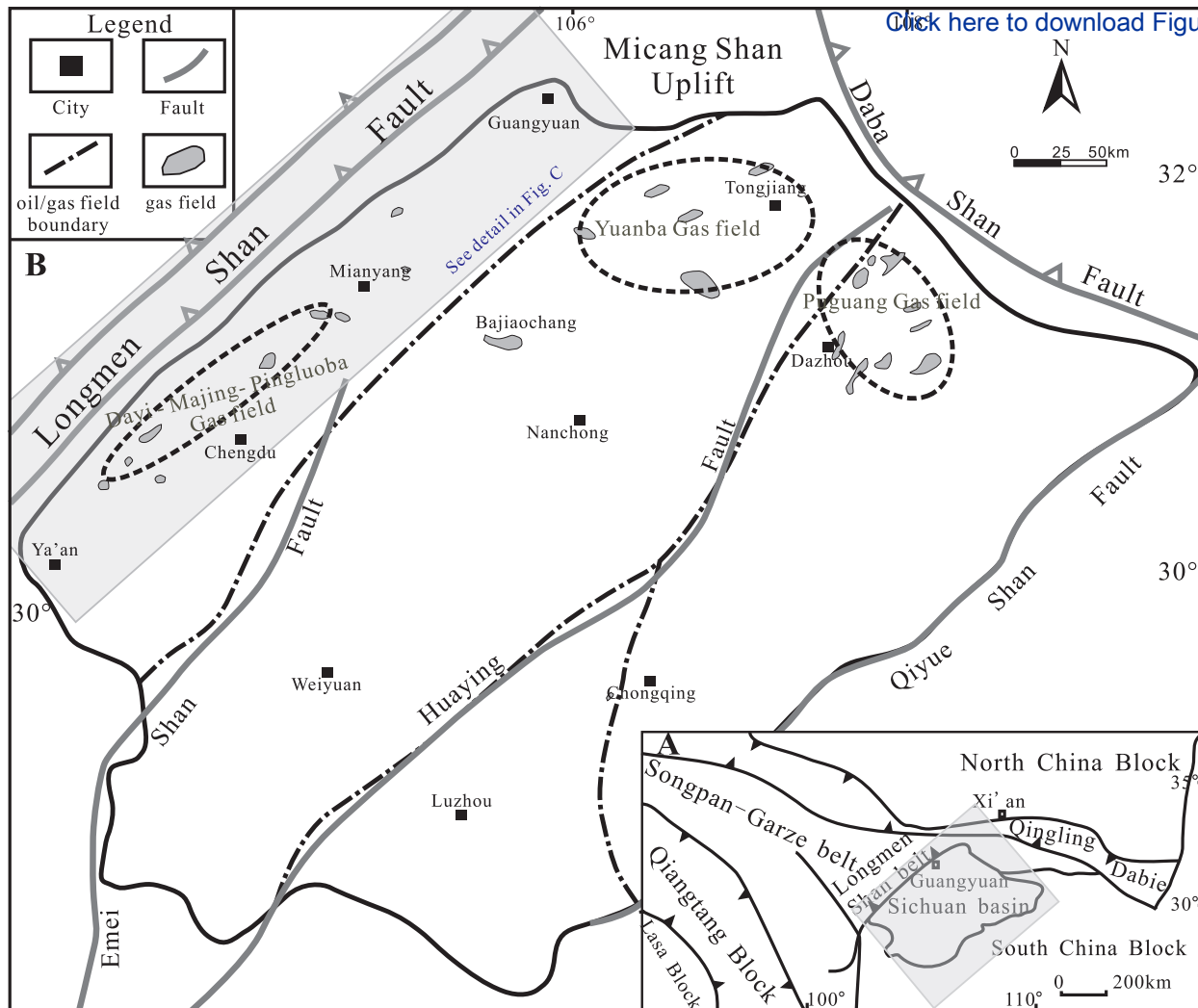
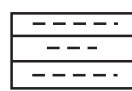


Figure 2

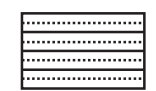
Period (Ma)		Formation	Symbol	Lithology	Thickness (m)	Petroleum system	Tectonic cycle	
Quaternary	2.6		Q				late	Himalayan
Neogene	23	Dayi	Nd				early	
Paleogene	66	Min Shan	Em		500-2000			
Cretaceous	145	Guankou	K <sub>2</sub> g				late	Yanshan
		Jiaguan	K <sub>1</sub> j			Seal		
Jurassic	163	Lianhuakou	J <sub>3</sub> l		650-1300		middle	
		Suining	J <sub>2</sub> sn			Seal		
		Shaximiao	J <sub>2</sub> s		200-1500		early	
		Qianfoyan	J <sub>1</sub> q			Reservoir		
Triassic	201	Baitianba	J <sub>1</sub> b		80-200	Reservoir		Indosinian
		Upper Xujiahe	T <sub>3</sub> X <sup>3-4</sup>				late	
		Lower Xujiahe	T <sub>3</sub> X <sup>1-2</sup>		250-2000		middle	
		Leikoupo	T <sub>2</sub>		60-1000		early	
Permian	253	Feixianguan	T <sub>1</sub> f		463-630	Reservoir		Hercynian
		Dalong	P <sub>2</sub> d		32-40	Source		
		Changxing	P <sub>2</sub> c		70-80	Reservoir		
		Maokou	P <sub>1</sub> m		97-225	Reservoir		
Carboniferous	299	Qixia	P <sub>1</sub> q		70-128	Reservoir		Hercynian
		Huanglong	C <sub>2</sub> h		0-276			
Devonian	359	Devonian	D <sub>2-3</sub>					Caledonian
		Pingyipu	D <sub>1</sub> p			Seal		
Silurian	419	Silurian	S			Reservoir		
Ordovician	443	Ordovician	O					
Cambrian	485	Changjianggou (sample layer)	Є <sub>1</sub> c		>225	Reservoir (sample layer)		Hercynian
		Qiongzhusi	Є <sub>1</sub> q		91-360	Source		
Precambrian	541	Doushantuo	Zd			Source		



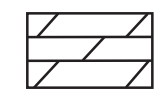
mudstone



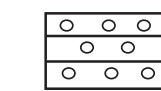
shale



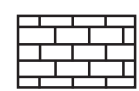
sandstone



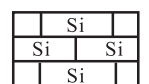
dolomitite



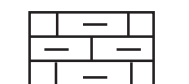
conglomerate




limestone



siliceous limestone



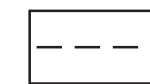
argillaceous limestone



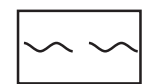
coarse siltstone



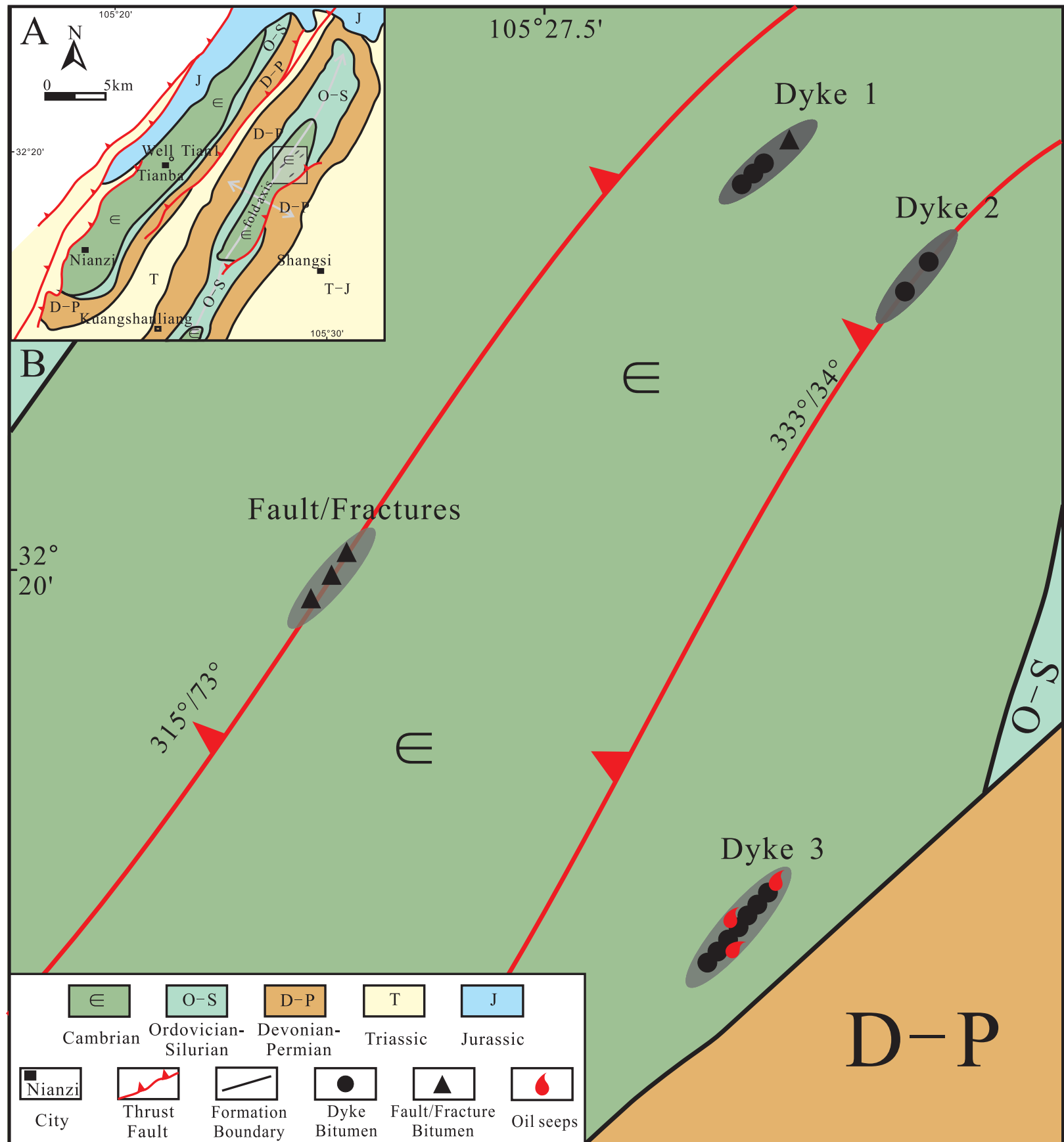
fine siltstone



disconformity



unconformity





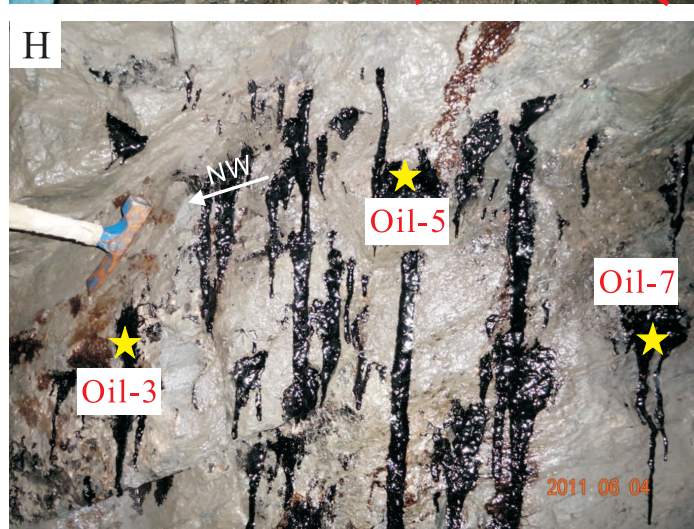
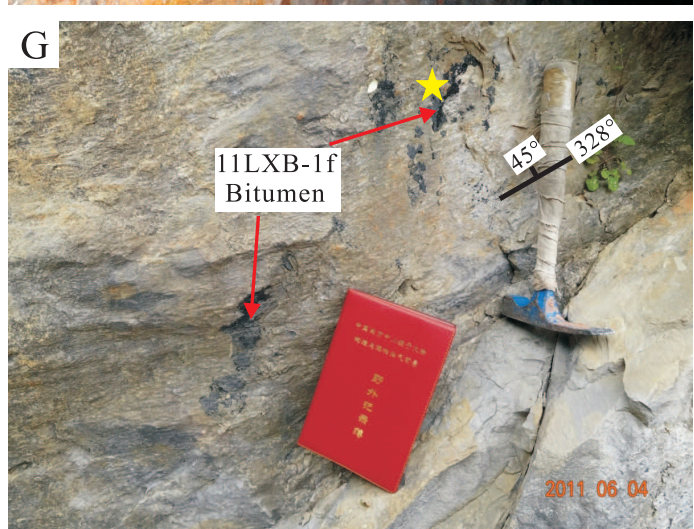
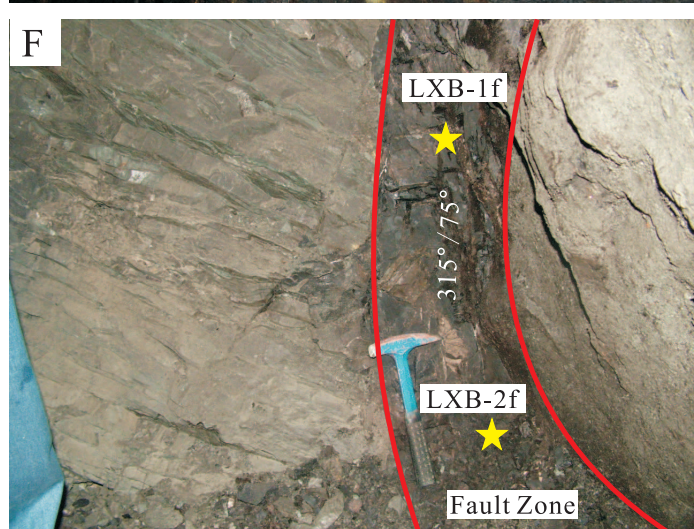
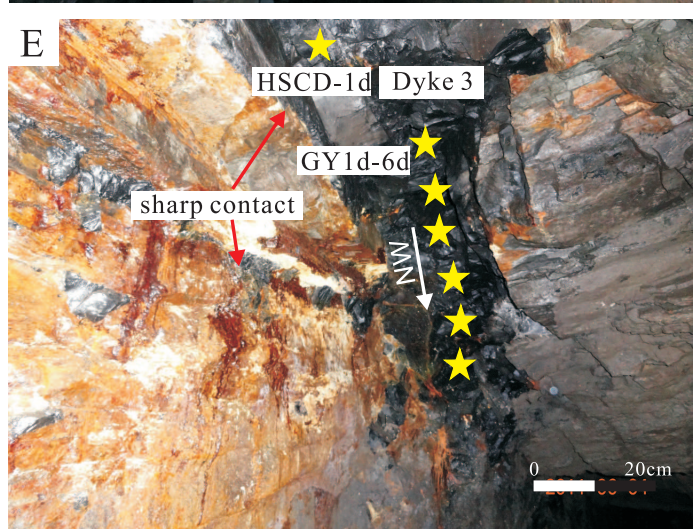
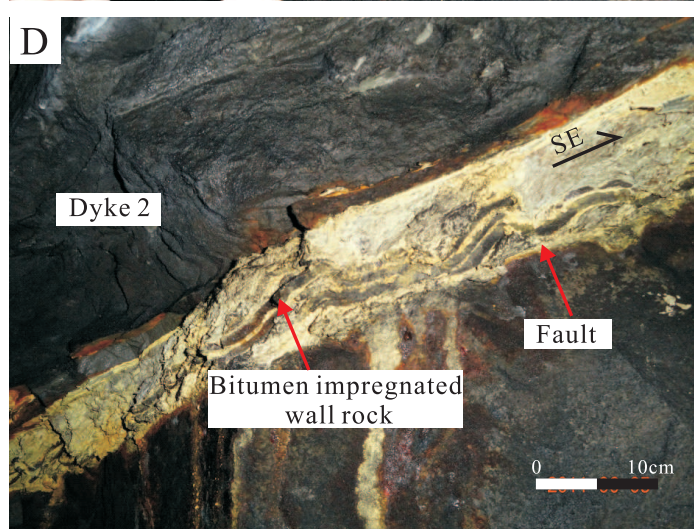
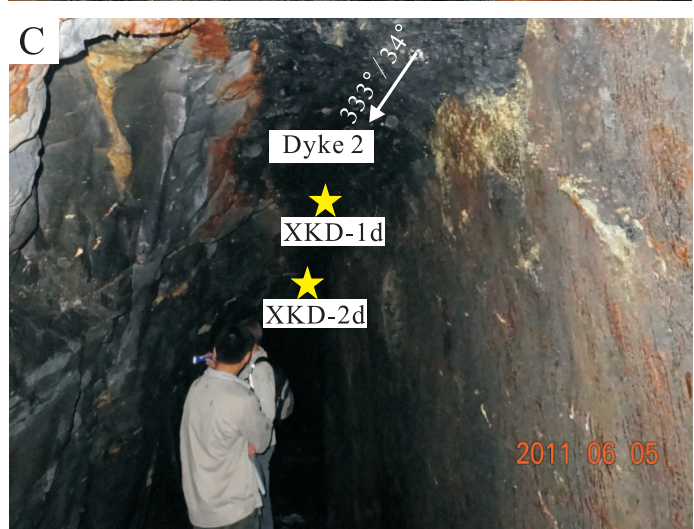
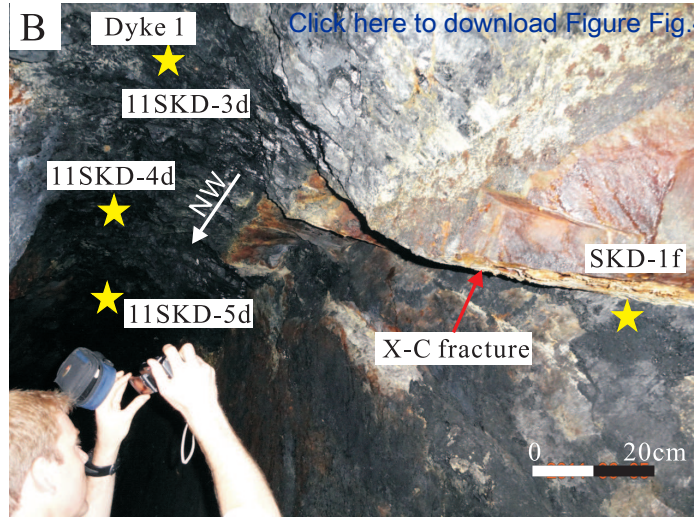
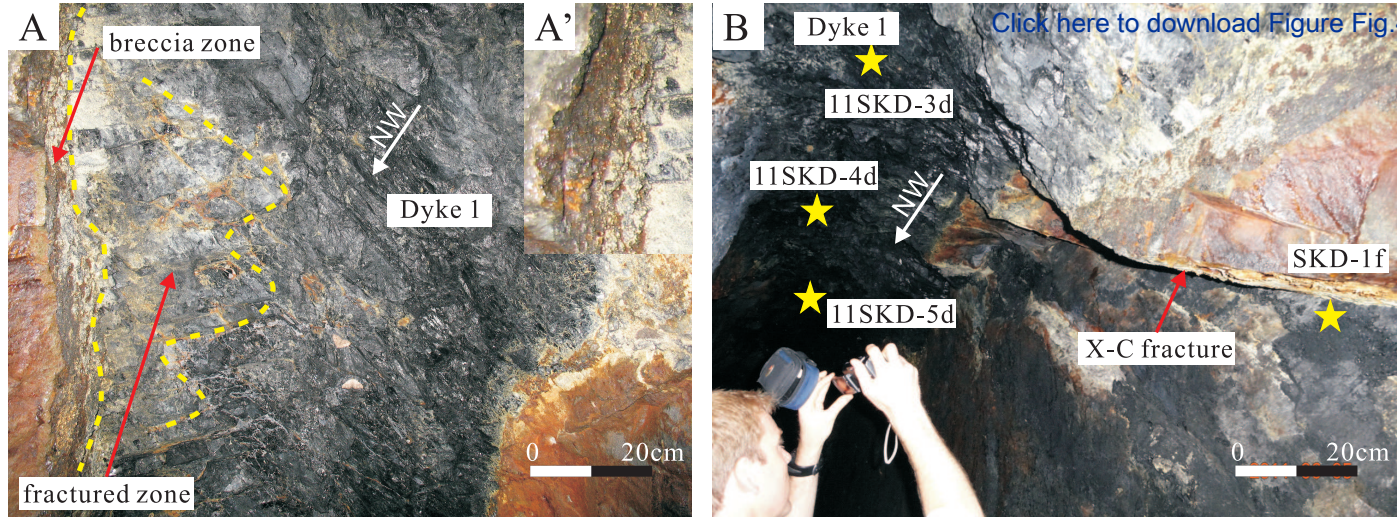


Figure 5

[Click here to download Figure Fig.5.eps](#)

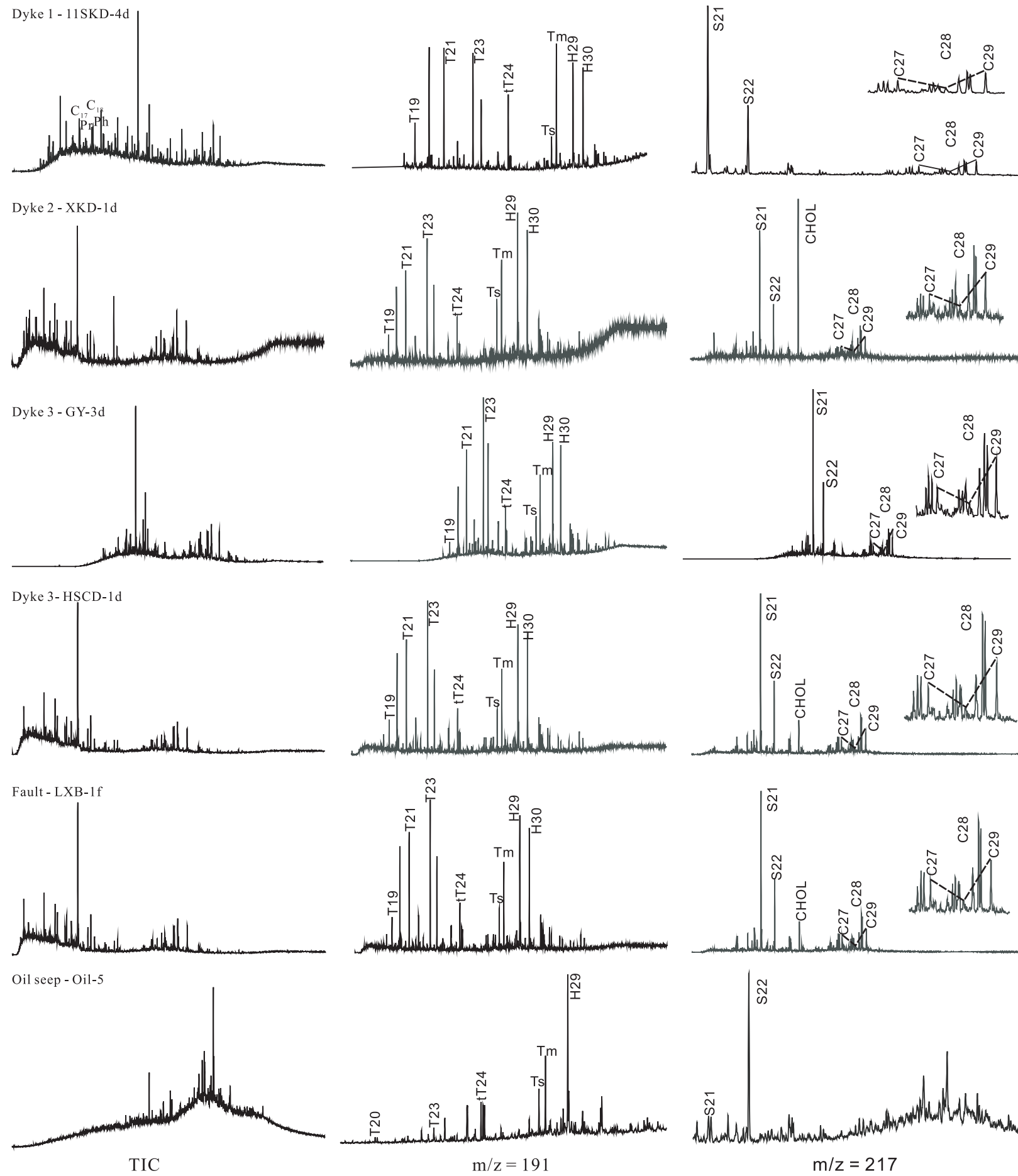
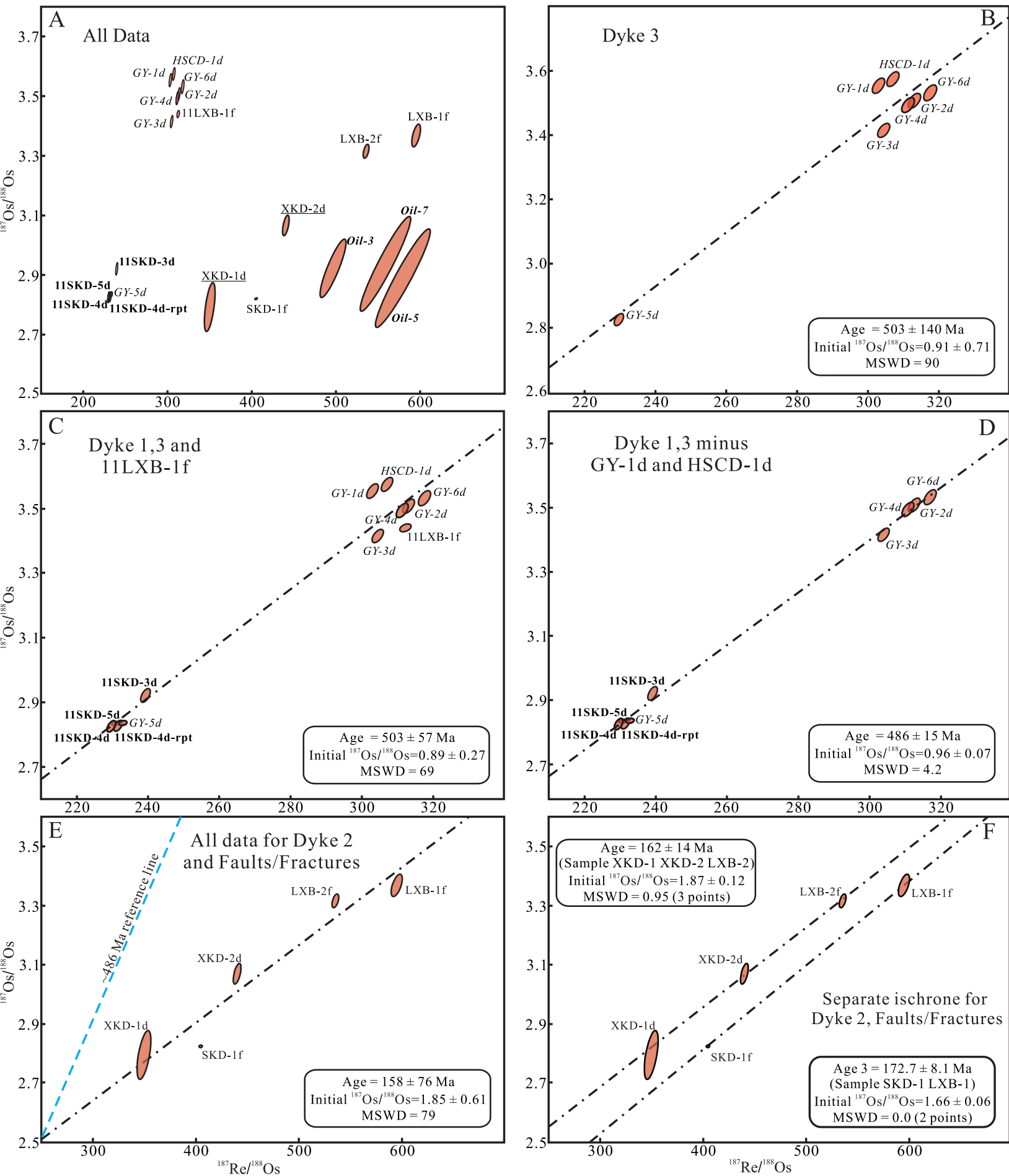


Figure 6

[Click here to download Figure Fig.6.eps](#)

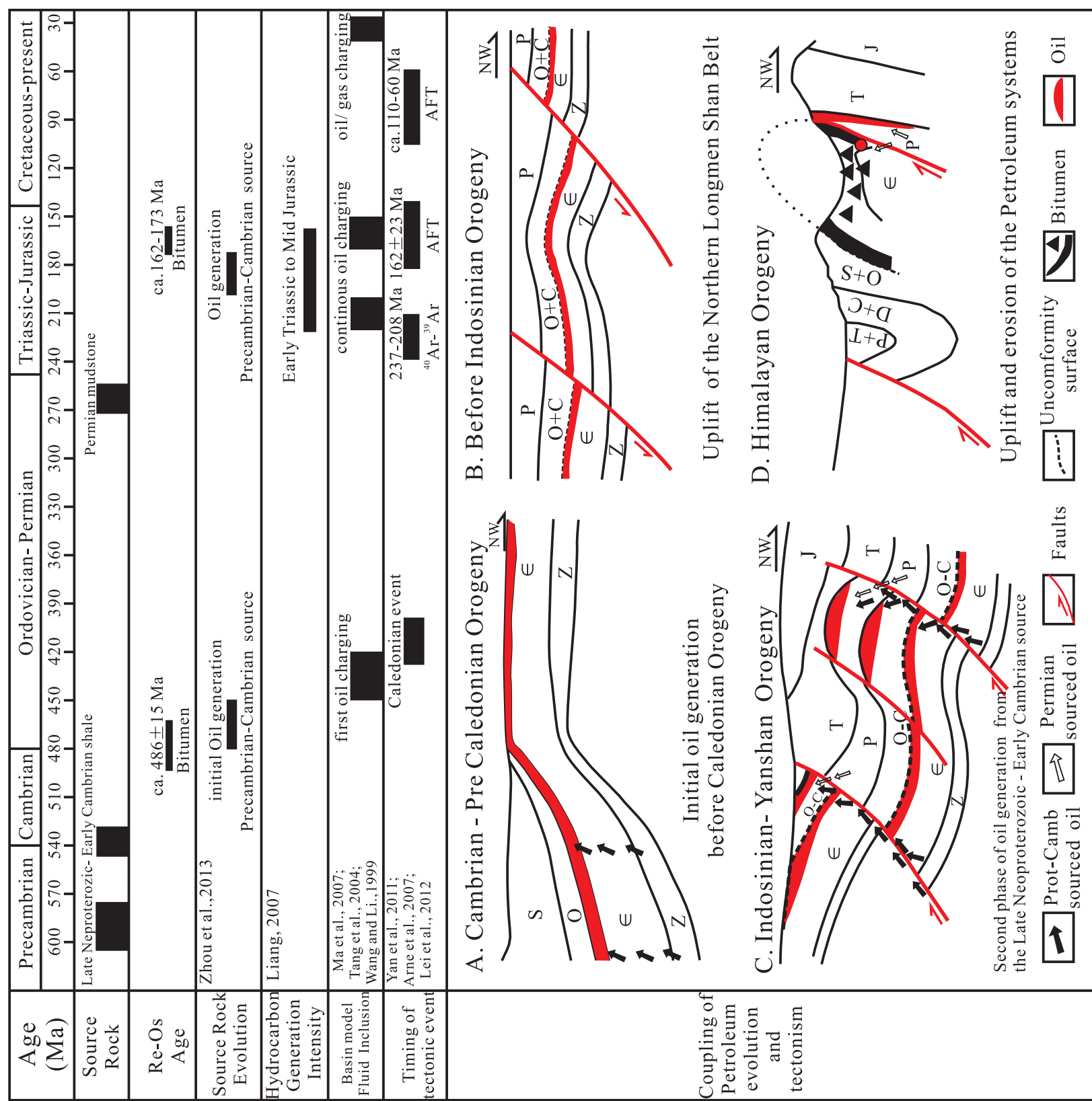


Table 1. The biomarker characteristics of the bitumen and present day oil seeps from the Kuangshangliang area, Northern Longmen Shan Thrust Belt

Sample name	ASPH (%)	CPI	Pr/C17	Ph/C18	Pr/Ph	GAM /H30	Ts/Ts+Tm	TR23/TR21	TR23 /tT24	tT24/TR26	DH30 /H30	H32 S/(R+S)	NOR25H /H30	S21/S22	C27R (%)	C28R (%)	C29R (%)	C29S /(S+R)	C29 $\beta\beta$ /( $\beta\beta$ + $\alpha\alpha$ )
<b>Dyke 1</b>																			
11SKD-4d	/	/	0.96	1.71	0.72	0.14	0.2	0.90	1.50	2.32	0.06	0.6	0.16	2.55	34.5	19.5	46	0.5	0.49
<b>Dyke 2</b>																			
XKD-1d	98	1.05	0.4	1.05	0.47	0.22	0.38	1.45	2.41	1.21	0.08	0.57	0.14	2.58	24.8	15.7	59.5	0.51	0.51
<b>Dyke 3</b>																			
GY-1d	/	1.04	/	/	/	0.18	0.32	1.67	2.85	1.03	0.05	0.54	0.16	2.41	30.1	15.2	54.7	0.52	0.53
GY-3d	/	1.16	/	/	/	0.19	0.32	1.57	2.88	1	0.05	0.56	0.16	2.42	27.7	14.4	57.9	0.5	0.53
GY-5d	/	0.91	/	/	/	0.13	0.31	1.31	2.20	1.43	0.05	0.58	0.17	2.5	30.4	16.2	53.4	0.52	0.55
HSCD-1d	99	2.59	0.7	0.91	0.95	0.15	0.35	1.49	3.01	1.06	0.05	0.62	0.13	2.45	32.2	16.3	51.5	0.47	0.57
<b>Fault and fractures</b>																			
SKD-1f	98	0.94	/	/	/	0.12	0.24	1.00	1.28	2.61	0.02	0.6	0.07	2.46	29	15.2	55.7	0.46	0.5
11LXB-1	99	1.21	/	/	/	0.17	0.32	1.38	2.82	1.01	0.05	0.6	0.17	2.26	30.8	16	53.2	0.47	0.55
LXB-1f	98	0.35	/	/	/	0.18	0.33	1.38	2.83	1.00	0.06	0.58	0.19	2.32	31.90	14.80	53.40	0.46	0.55
<b>Oil</b>																			
Oil-3	13.54	/	/	/	/	7.59	0.37	/	/	0.51	5.54	/	/	0.21	/	/	/	/	/
Oil-5	9.48	/	/	/	/	3.91	0.36	/	0.26	0.52	3.1	/	/	0.2	/	/	/	/	/

Table 2. Re-Os elemental and isotopic data of the bitumen and present day oil seeps from the Kuangshanliang area, Northern Longmen Shan Thrust Belt.

Sample	latitude	longitude	Re (ppb)	Re blk %	Os (ppt)	Os blk %	<sup>187</sup> Re/ <sup>188</sup> Os	<sup>187</sup> Os/ <sup>188</sup> Os	rho	Osi <sub>503</sub>	Osi <sub>486</sub>	Osi <sub>483</sub>	Osi <sub>158</sub>
<b>Dyke 1</b>													
11SKD-3d	32°20'27"	105°27'47"	403.5(1.0)	0.004	11094.0(64.7)	0.007	239.1(1.1)	2.92(0.02)	0.560	/	/	0.99	/
11SKD-4d	32°20'25"	105°27'48"	512.2(1.8)	0.003	14478.3(46.3)	0.006	230.7(0.9)	2.84(0.01)	0.260	/	/	0.97	/
11SKD-4d-rpt	32°20'25"	105°27'48"	518.8(1.3)	0.010	14605.3(75.8)	0.046	231.5(1.0)	2.83(0.01)	0.567	/	/	0.96	/
11SKD-5d	32°20'26"	105°27'47"	547.9(1.9)	0.009	15347.3(50.3)	0.042	232.8(0.9)	2.84(0.01)	0.238	/	/	0.96	/
<b>Dyke 2</b>													
XKD-1d	32°20'26"	105°27'49"	332.9(1.1)	0.007	6182.4(80.9)	0.107	349.7(5.2)	2.79(0.07)	0.591	/	-0.05	/	1.87
XKD-2d	32°20'25"	105°27'49"	334(1.2)	0.007	5058.7(38.4)	0.133	440.2(3.2)	3.07(0.03)	0.576	/	-0.51	/	1.91
<b>Dyke 3</b>													
GY-1d	32°19'21"	105°27'47"	305.6(0.8)	0.008	7033.5(40.5)	0.012	302.9(1.3)	3.56(0.02)	0.581	1.01	/	1.11	/
GY-2d	32°19'20"	105°27'45"	320.3(0.8)	0.007	7105.0(40.4)	0.012	313.1(1.4)	3.51(0.02)	0.582	0.87	/	0.98	/
GY-3d	32°19'22"	105°27'47"	303.7(0.8)	0.008	6869.0(38.1)	0.012	304.4(1.3)	3.42(0.02)	0.577	0.85	/	0.96	/
GY-4d	32°19'21"	105°27'46"	293.5(0.7)	0.008	6538.1(37.2)	0.013	311.3(1.4)	3.49(0.02)	0.577	0.88	/	0.98	/
GY-5d	32°19'22"	105°27'47"	524.8(1.3)	0.005	14895.1(79.1)	0.005	229.5(1.0)	2.83(0.01)	0.562	0.89	/	0.97	/
GY-6d	32°19'20"	105°27'48"	329.3(0.8)	0.007	7216.8(42.4)	0.012	317.6(1.4)	3.53(0.02)	0.567	0.86	/	0.97	/
HSCD-1d	32°19'21"	105°27'47"	284.1(0.7)	0.006	6464.5(36.3)	0.013	307.0(1.3)	3.58(0.02)	0.581	0.99	/	1.10	/
<b>Fault and Fracture</b>													
11LXB-1f	32°20'07"	105°27'20"	311.1(1.1)	0.005	6875.7(29.5)	0.013	312.2(1.3)	3.44(0.01)	0.408	/	/	/	/
SKD-1f	32°20'26"	105°27'47"	525.9(1.8)	0.004	8460.4(20.0)	0.074	404.8(1.4)	2.82(<0.01)	0.468	/	-0.47	/	1.75
LXB-1f	32°20'06"	105°27'19"	352.2(1.2)	0.005	4058.2(31.6)	0.413	595.1(4.2)	3.37(0.03)	0.582	/	-1.47	/	1.80
LXB-2f	32°20'06"	105°27'20"	334.4(1.1)	0.007	4259.3(25.6)	0.409	535.6(2.8)	3.32(0.02)	0.505	/	-1.04	/	1.90
<b>Oil</b>													
Oil-3	32°19'20"	105°27'48"	9.6(0.1)	0.185	127.2(1.9)	3.803	496.3(12.6)	2.92(0.08)	0.88	/	/	/	/
Oil-5	32°19'21"	105°27'47"	8.1(0.1)	0.312	91.7(2.0)	3.632	579.3(26.6)	2.89(0.14)	0.948	/	/	/	/
Oil-7	32°19'20"	105°27'46"	7.7(0.1)	0.308	90.3(1.9)	3.460	558.6(24.5)	2.94(0.13)	0.947	/	/	/	/

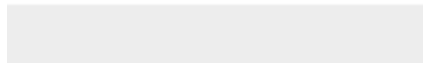
Note: asphaltene fraction of the oil were first precipitated using 40 times volume of *n*-heptane (~1 g oil with 40 ml solvent) at room temperature for at least 8 hrs and Re-Os analyses are conducted on the asphaltenes.



[Click here to access/download](#)

**Dataset**

[appendix Re-Os data table 20170227.xlsx](#)







# AAPG | BULLETIN

## Transfer of Copyright Agreement

Copyright including rights in transmissions is hereby transferred to The American Association of Petroleum Geologists (for government employees: to the extent transferable), effective if and when the work is accepted for publication. A "transmission" for purposes of this agreement is defined as a reproduction distributed by any device or process whereby a copy of the work is fixed beyond the place from which it was sent.

Copyright to: *AAPG Bulletin (The American Association of Petroleum Geologists)*

Name of Authors: *Xiang Ge, Chuanbo Shen, David Selby, Jie Wang, Liangbang Ma, Xiaoyan Ruan, Shouzhi Hu, Lianfu Mei*

DOI:

To be signed by an author (who agrees to inform the others, if any) or, in the case of a "work made for hire," by the employer.

Chuanbo Shen

Signature

Printed Name

China University of Geosciences(Wuhan)

Title (if not author)

Company or Institution

2/22/2017

Date

Issue: Volume/Number (Month, Year)